RESEARCH ARTICLE



Disentangling natural vs. anthropogenic induced environmental variability during the Holocene: Marambaia Cove, SW sector of the Sepetiba Bay (SE Brazil)

Wellen Fernanda Louzada Castelo ¹ • Maria Virgínia Alves Martins ^{2,3} • Michael Martínez-Colón ⁴ • Josefa Varela Guerra ⁵ • Tatiana Pinheiro Dadalto ⁶ • Denise Terroso ³ • Maryane Filgueiras Soares ² • Fabrizio Frontalini ⁷ • Wânia Duleba ⁸ • Orangel Antonio Aguilera Socorro ⁹ • Mauro Cesar Geraldes ² • Fernando Rocha ³ • • Sergio Bergamaschi ²

Received: 24 July 2020 / Accepted: 21 December 2020 © The Author(s), under exclusive licence to Springer-Verlag GmbH, DE part of Springer Nature 2021

Abstract

Multiproxy approach based on textural, mineralogical, geochemical, and microfaunal analyses on a 176-cm-long core (SP8) has been applied to reconstruct the Holocene paleoenvironmental changes and disentangling natural vs. anthropogenic variability in Marambaia Cove of the Sepetiba Bay (SE Brazil). Sepetiba Bay became a lagoonal system due to the evolution and development of the Marambaia barrier island during the Holocene and the presence of an extensive river basin. Elemental concentrations from pre-anthropogenic layers from the nearby SP7 core have been used to estimate the baseline elemental concentrations for this region and to determine metals enrichment factors (EF), pollution load index (PLI), and sediment pollution index (SPI). Record of the core SP8 provides compelling evidence of the lagoon evolution differentiating the effects of potentially toxic elements (PTEs) under natural vs. anthropic forcing in the last ~9.5 ka BP. The study area was probably part of coastal sand ridges between \approx 9.5 and 7.8 ka BP (radiocarbon date). Events of wash over deposited allochthonous material and organic matter between \approx 8.6 and 7.8 ka, Climatic event 8.2 ka BP, in which the South American Summer Monsoon was intensified in Brazil causing higher rainfall and moisture was scored by an anoxic event. Accumulation of organic matter resulted in oxygen depletion and even anoxia in the sediment activating biogeochemical processes that resulted in the retention of potentially toxic elements (PTEs). After ≈ 7.8 ka BP at the onset of the Holocene sea-level rise, a marine incursion flooded the Marambaia Cove area (previously exposed to subaerial conditions). Environmental conditions became favorable for the colonization of benthic foraminifera. The Foram Stress Index (FSI) and Exp(H'bc) indicate that the environmental conditions turned from bad to more favorable since \approx 7.8 ka BP, with maximum health reached at ≈ 5 ka BP, during the mid-Holocene relative sea-level highstand. Since then, the

Responsible editor: Vedula VSS Sarma

Maria Virgínia Alves Martins virginia.martins@ua.pt

Wellen Fernanda Louzada Castelo wellenflc@yahoo.com.br

Michael Martínez-Colón michael.martinez@famu.edu

Josefa Varela Guerra josie.guerra@gmail.com

Tatiana Pinheiro Dadalto tpdadalto@gmail.com

Denise Terroso laraterroso@ua.pt

Maryane Filgueiras Soares maryane.filgueiras@hotmail.com

Fabrizio Frontalini fabrizio.frontalini@uniurb.it

Wânia Duleba wduleba@usp.br

Orangel Antonio Aguilera Socorro orangel.aguilera@gmail.com

Mauro Cesar Geraldes geraldes@gmail.com

Fernando Rocha tavares.rocha@ua.pt

Sergio Bergamaschi sergioberg7@hotmail.com

Extended author information available on the last page of the article



sedimentological and ecological proxies suggest that the system evolved to an increasing degree of confinement. Since ≈ 1975 AD, a sharp increase of silting, Cd, Zn, and organic matter also induced by anthropic activities caused major changes in foraminiferal assemblages with a significant increase of Ammonia/*Elphidium* Index (AEI), EF, and SPI values and decreasing of FSI and Exp(H'bc) (ecological indicators) demonstrating an evolution from "moderately polluted" to "heavily polluted" environment (bad ecological conditions), under variable suboxic conditions. Thus, core SP8 illustrates the most remarkable event of anthropogenic forcing on the geochemistry of the sediments and associated pollution loads and its negative effect on benthic organisms.

Keywords Multiproxies · Foraminifera · Metals · Ammonia/Elphidium Index · Foram Stress Index · Ecological Quality Status

Introduction

The accurate knowledge of coastal areas is a key point for understanding their evolution and change in response to natural factors and anthropic pressure. Today, the protection and management of coastal environments are important issues when considering that about 13% of the world's population lives in these areas and use their resources (Mc Granaham et al. 2007; Neumann et al. 2015). Recent studies have revealed a substantial worldwide decline in the estuarine ecosystem service and functioning (e.g., Kuniansky and Rodríguez 2010) because of their excessive socio-economic exploitation. Numerous efforts worldwide have therefore been made to understand estuarine resilience to anthropogenically induced stressors such as sewage discharge (e.g., Alegría et al. 2016) and the input of potentially toxic elements (PTEs) as defined by Martínez-Colón et al. (2009). Understanding the current environmental health of coastal areas is a major concern for resource managers, policy-makers, and stakeholders. The management and assessment of point and non-point sources of pollution are of great importance; however, the lack of pre-management or pre-impact conditions (i.e., reference or baseline) limits the understanding and the evaluation of current conditions, particularly in estuarine environments that are typically naturally stressed (i.e., Elliott and Quintino 2007; Bouchet et al. 2018).

Benthic foraminifera (protozoa, meiofaunal organisms) have been widely applied as effective bioindicators because of their high sensitivity, abundance, and specific ecological requirement in spatial and temporal studies in estuarine environments (e.g., Prazeres et al. 2020; Hess et al. 2020). Similarly, other coastal benthic organisms like microbes, nematodes, and microgastropods among others are also sensitive to environmental stressors such as changes in sediment supply, dissolved oxygen (DO), PTEs, organic matter, and pH (e.g., Hippensteel and Martin 1999; Olabarria 2002; Lai et al. 2005; Chakravarty and Banerjee 2008; Taheri et al. 2015; Hermans et al. 2017; Aylagas et al. 2016; Franzo et al. 2019). Differently from other meiofaunal groups, foraminifera can be preserved in the sediments because of their shell (test). This makes them very useful in recording the evolution of coastal environmental changes (e.g., sea-level variation, ocean productivity, paleoenvironmental reconstructions) (e.g., Smith et al. 2013; Waśkowska and Kaminski 2019) but, most importantly, in providing a proxy for historical reconstructions and the definition of reference conditions or the deviation from them (e.g., Alve 1991; Dolven et al. 2013; Martínez-Colón et al. 2017; Hess et al. 2020).

Estuaries are highly dynamic environments where water column stratification, organic matter flocculation, oxygenation, and salinity changes among others are just a few of the processes that alter the physiochemical characteristics of these ecosystems (Wolanski et al. 2009; Silva et al. 2015). Mechanical alterations like dredging may create permanent haloclines and oxiclines in the water column that might negatively impact the bottom sediments, influence the fate and transport of PTEs, and the biota living therein (e.g., Martínez-Colón et al. 2018). On the other hand, spit and bay barrier development/migration also alter the overall characteristics of an estuary by promoting changes in the sediment texture and water chemistry (e.g., Lessa et al. 1998; Miselis et al. 2016). Disentangling natural and anthropogenic induced alterations in surface estuarine sediments is a very important task though quite challenging. Sediment core provides a window, in time, to assess the natural variability of an ecosystem, and offers the opportunity to define baseline conditions. Several ecological and paleoecological studies have applied benthic foraminifera in paleoenvironmental reconstruction in the Sepetiba Bay (e.g., Tinoco 1967; Zaninetti et al. 1976, 1977; Suguio et al. 1979; Brönnimann et al. 1981a, 1981b; Dias-Brito et al. 1988; Laut et al. 2012; Pinto et al. 2016, 2017; Alves Martins et al. 2019a, 2020). These works have documented the main benthic foraminiferal species and factors that contribute the most to their distribution. Indeed, they have also revealed Holocene paleoenvironmental changes that have been associated with sea-level oscillations or recent environmental changes related to anthropic pressures in this ecosystem.

The present work aims to identify natural and anthropic factors that influenced the Holocene environmental evolution of the external sector of Sepetiba Bay (SE Brazil) by using benthic foraminifera as bioindicators and sedimentological data.



Study area

The Sepetiba Bay is located on the main economic axis of Brazil (Rio de Janeiro, São Paulo) between latitudes 22° 53′ S and 23° 05′ S and longitudes 44° 01′ W and 43° 33″ W, about 50 km west of the city of Rio de Janeiro (Fig. 1a). The bay basin mostly comprises Precambrian rocks, such as migmatites, gneisses, and gneisses-granitoid from the Occidental, Oriental, and Paraiba do Sul Terrains (Tupinambá et al. 2007). It also contains some felsic alkaline intrusive rock bodies such as the Tinguá and Mendanha massifs (Geraldes et al. 2013, 2017) and coastal massifs, such as Ilha Grande, Marambaia, Jaguanum, Itacuruçá Islands, and Pedra Branca (Nascimento et al. 2019); quaternary fluvial deposits; and fluvio-marine sediments that are drained by rivers (Misumi et al. 2014; Rodrigues et al. 2018).

The Sepetiba Bay covers an area of 520 km² and spans 170.5 km in perimeter (SEMADS 2001). The bay is bordered by the Serra do Mar massif on the northern and eastern sides, and the Marambaia barrier island at the south (Fig. 1). The Marambaia barrier island, mostly represented by quaternary sediments, gives a semi-elliptical shape to the bay and protects it from high-energy waves (Lacerda et al. 2001) making the bay a semi-confined lagoon. The contact with the ocean mostly occurs towards the western sector, between the islands of Itacuruçá and Jaguanum.

The bay's watershed has an area of 2654 km² and is divided into three sub-basins (Guandu River, Guarda River, and Guandu-Mirim River) representing about 70% of the total area of the basin that drains into the Sepetiba Bay (SEMADS 2001; Misumi et al. 2014). The Guandu River basin includes 123 rivers having an average flow of about 22 m³/s and strongly contributes to the input of fresh water into the bay (PARH Guandu 2010). The highest average flow is registered from November to January when it reaches its maximum peak at 42.1 m³ s⁻¹ (PARH Guandu 2010).

The region is characterized by a hot-humid climate with average rainfall ranging between 1200 and 2500 mm year⁻¹ (Lacerda et al. 2001, SEMADS 2001). In the external sector of the Sepetiba Bay, surface water salinities between 33.8 and 35.7 can be recorded, but they decrease eastwards towards the innermost region of the bay due to the contribution of freshwater from rivers (Miranda et al. 1977). Water temperatures have been recorded ranging between 20 and 27.5 °C (Gutierrez et al. 2011).

The water circulation in Sepetiba Bay is mainly controlled by tidal and wind actions (Cunha et al. 2001, 2006; Copeland et al. 2003). The predominant wind regime is from south and west–southwest and secondarily from the north–northeast and east–northeast, depending on the season, with estimated average velocities ranging from 1.5 to 5.0 m s⁻¹ (SEMADS 2001). The flood and ebb tidal currents strongly control the mixing of

oceanic water masses and the inner lagoonal low salinity waters (Duque et al. 2008).

The bottom sediments of the Sepetiba Bay have been studied by several authors who have reported sandy sediments at the entrance and in the main channels of the bay where the bottom currents are more hydrodynamic (e.g., Barcellos et al. 1997; Carelli et al. 2011; Roncarati and Carelli 2012; Nascimento et al. 2013; Borges and Nittrouer 2016). In this region, the sedimentary budget is strongly controlled by the entry of allochthonous materials coming from surface runoff. The stratigraphic packages of the Sepetiba Bay area represent interbedding between fluvio-terrestrial and coastal-marine sediments (Friederichs et al. 2013; Reis et al. 2020). The sea-level variations throughout the Quaternary and, particularly in the late Holocene, played a major role in the fate and transport of sediments and on the coastal evolution of the bay (e.g., Borges and Nittrouer 2016; Pinto et al. 2017; Alves Martins et al. 2020; Reis et al. 2020).

Materials and methods

This work is based on the study of the core SP8 (176 cm long; 23° 02′ 45" S and 43° 54′ 15" W - UTM 2549032.1418914 / 387750.75373566 - WGS84) collected at a depth of 2.2 m, about 1.8 km from the west bank of Ponta da Pombeba, in the Marambaia Cove that is in the eastern region of Sepetiba Bay (SE Brazil; Fig. 1a). This work also considers additional elemental concentrations (used as baseline values) from the SP7 core (108 cm long; 23° 02′ 36.373" S and 43° 44′ 02.015" W -UTM 2548871.2920853/370330.80324905 - WGS84) collected at a depth of 3 m, near the eastern margin of the Marambaia barrier island close to Guaratiba area. Both cores were collected by SCUBA divers using piston percussion methods and PVC pipes (160 cm in diameter) in June 2015. In the laboratory, the cores were opened, described, and sampled at 2 cm resolution. Samples were dried (≈ 50 °C) for subsequent textural, mineralogical, geochemical, and microfaunal analyses.

Radiocarbon dating

For radiocarbon (¹⁴C) analyses, mollusk shells and fragments were sampled in the layers 36–38 cm, 100–102 cm, and 132–134 cm and a fragment of wood at horizon 148–150 cm for the core SP8 and mollusk shells were also sampled at 41 cm downcore for the SP7 core. All analyses were carried out within the scope of the work developed by Dadalto (2017), at the National Ocean Sciences Accelerator Mass Spectrometry laboratory (NOSAMS/WHOI; Woods Hole Oceanographic Institution, USA). The ¹⁴C dating results are presented in ages (years) before the present (BP). The ages



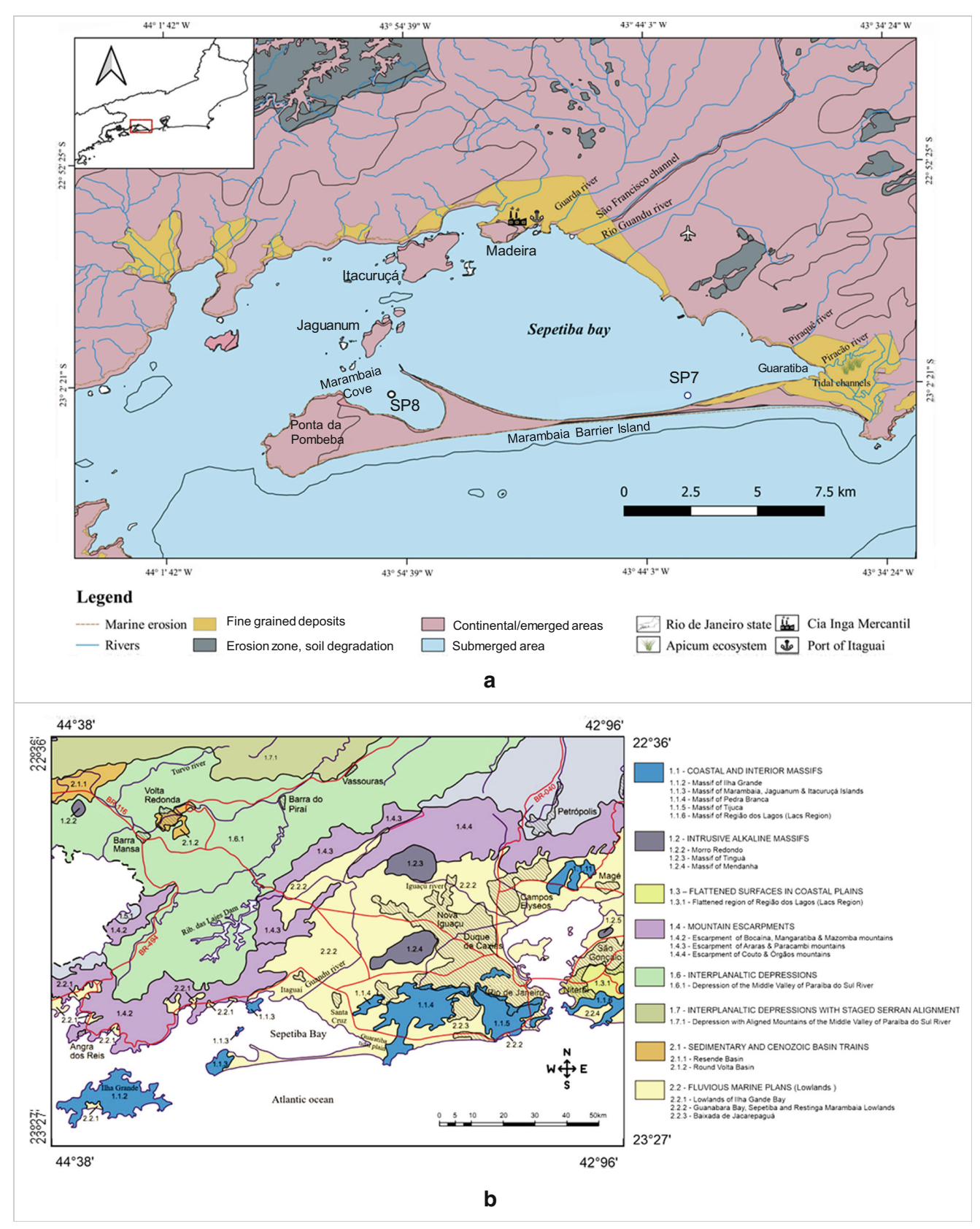


Fig. 1 a Location of cores SP8 and SP7 in the Sepetiba Bay (SE Brazil). b Map of the main geomorphological units of Rio de Janeiro State (adapted from Dantas 2000)



were calibrated against the SHCAL database of Hogg et al. (2013) that is designed for the Southern Hemisphere using CALIB ¹⁴C, an online program (http://calib.org/calib/) (Stuvier and Reimer 1993; Stuiver et al. 2020).

The impact of coastal dynamics on the radiocarbon (14 C) marine reservoir effect (MRE) in the State of Rio de Janeiro was recently analyzed by Macario et al. (2018). These authors reported that, in the region, the ΔR values present temporal or spatial variations due to ocean dynamics, continental input, and the choice of marine organisms used for ΔR determination. Macario et al. (2018) found a negative value of ΔR at about 3 ka of Ilha Grande island, for a shell mound. Therefore, it was decided to not introduce any value of ΔR to the calibrated values of 14 C.

Textural and mineralogical analyses

For the granulometric analysis, about 15 g per sample were used. Wet sieving was done to separate the fine ($< 63 \mu m$) from the coarse (> 63 µm) fractions. After subsequent drying and reweighing, the > 63- μ m fraction was dry sieved (125 μ m, 250 μm, 500 μm). All sediment sizes are represented as a percentage of each size fraction. The textural parameters and categorization were based on the classification by Folk and Ward (1957). The mineralogical analyses were performed in the fine fraction (< 63 μm) by X-ray diffraction, according to the methodology described by Martins et al. (2007). Textural and mineralogical data were acquired aiming to identify energetic changes in the sedimentary environment and variations in the composition of the sediment. Silt and clay fraction mineralogy and geochemistry have been used for sedimentological and paleoenvironmental analysis since the 1960s (e.g., Biscaye 1965) until present. This fine fraction, since it has greater mineralogical and geochemical variability than coarser fractions or bulk sediments, provides a higher sensitive proxy for paleoenvironmental and provenance studies (Fagel 2007; Trindade et al. 2010; Hofer et al. 2013).

Organic matter and carbonate analyses

The total organic matter (TOM) content was determined by weight loss for each dry sediment sample, after being subjected to a chemical digestion treatment using hydrogen peroxide (H₂O₂ at 20%) at 60 °C for 24h, followed by sequential washing, drying, and reweighing of the sediment. The residual digested sediments from the TOM analysis were then leached in 10% hydrochloric acid for one hour to determine the carbonate content (CO₃). Intermediate washes with distilled water and reweighing were done to reach a stable weight indicative of total CO₃ dissolution (Krumbein and Pettijohn 1938). Both TOM and CO₃ values are presented as percentages. Although the reaction of organic matter with H₂O₂ can partially destroy the carbonates its presence was also estimated by X-ray diffraction (XRD) techniques. It was found that the content of calcite (by XRD), carbonates, and Ca is coherent,

as seen in the "Results" section. All these variables have similar trends and can therefore indicate the same conditions.

Elemental analyses

The elemental analyses from the core SP7 and SP8 were performed by inductively coupled plasma-mass spectrometry (ICP-MS) at the Acme Analytical Laboratories (Bureau Veritas LTDA, Vancouver, Canada). The preparation of each sample consisted of macerating 5 g of bulk sediment using an agate mortar/pestle and subsequently dry sieving (< 63 μm). To ensure no cross-contamination, the mortar/pestle and sieve were cleaned with distilled water and dried between each sample. All sediment samples were leached using a modified aqua regia solution (1:1:1 HNO₃/HCl/H₂O) (http://acmelab.com/). Some elements (i.e., As, Cd, Co, Cr, Cu, Hg, Ni, Pb, Zn) were used to determine anthropogenic impacts while others (i.e., Al, Ca, Mg, Mn, Mo, Sc, Sr, Ti, and U) were considered to assess the paleoenvironmental evolution of the bay.

The enrichment factor for each analyzed chemical element was calculated following Buat-Menard and Chesselet (1979):

$$EF = \frac{\left(\frac{Cx}{Cn}\right) Environment}{\left(\frac{Cx}{Cn}\right) Baseline}$$

where Cx is the element concentration for which it is intended to determine the enrichment; Cn is the concentration of the normalizing (baseline) element. Scandium (Sc) was used as a normalizing element (see explanation in the "Results" section). The local elemental baseline values were derived for the mean elemental concentrations in 6 layers (between 50 and 106 cm of the SP7 core) that were deposited before 8100 ± 480 BP (conventional radiocarbon age of a mollusk shell obtained in the 41 cm core layer) (Appendix 1). The mean elemental concentrations of SP7 core (in non-anthropized sediments, as indicated the 14C data obtained, in a shell, at the level of 41 cm, with a conventional radiocarbon age of 8100 ± 480 years BP; see 3.1 item) were selected as baseline values since they were analyzed in the same laboratory and with the same methodology (Appendix 1; Table 1). The EF classification (Table 2) was based on Sutherland (2000). For Mo and U, the EF values also were calculated by normalizing with Sc. However, the average shale concentration as reported by Turekian and Wedepohl (1961) was used for these elements (including Sc) for comparison with published data.

The sediment pollution index was calculated according to Singh et al. (2002) by the equation:

$$SPI = \frac{\sum (EF_{m} \times W_{m})}{\sum W_{m}}$$

where EFm is the PTE enrichment factor in the sample; $W_{\rm m}$ is the PTE toxicity weight. The $W_{\rm m}$ values are as follows: 1 for



Table 1 Baseline concentrations used to determine de EF values of chemical elements analyzed in core SP8

Elemer	nt concentrations	3	Elemen	Element concentrations					
Al	%	3.8	Mn	mg kg ⁻¹	112.3				
As	${\rm mg~kg^{-1}}$	5.7	Mo ^a	$\rm mg~kg^{-1}$	5.9/2.6 ^a				
Ca	%	0.1	Ni	${ m mg~kg}^{-1}$	6.4				
Cd	${\rm mg~kg^{-1}}$	0.1	Pb	${ m mg~kg}^{-1}$	43.8				
Co	${\rm mg~kg^{-1}}$	2.5	Sc	${ m mg~kg}^{-1}$	5.2/13 ^a				
Cr	${\rm mg~kg^{-1}}$	45.0	Sr	${ m mg~kg}^{-1}$	27.7				
Cu	${\rm mg~kg^{-1}}$	7.1	Ti	%	0.012				
Hg	${\rm mg~kg^{-1}}$	0.3	U^a	${\rm mg~kg^{-1}}$	6.3/3.7 ^a				
Mg	%	0.4	Zn	$mg\;kg^{-l}$	38.4				

^a Baseline values from shales as reported by Turekian and Wedepohl (1961)

Cr and Zn; 2 for Ni and Cu; 5 for Pb and; 300 for Cd (Singh et al. 2002). The SPI values were categorized by Singh et al. (2002) (Table 2).

The pollution load index was calculated using the equation of Tomlinson et al. (1980):

$$PLI = \sqrt[n]{CF1 \cdot CF2 \cdot CF3 \cdot \dots \cdot CFn}$$

where CF is the contamination factor for each PTE (As, Cd, Co, Cr, Cu, Hg, Ni, Pb, and Zn) and was calculated as Cs/Cb (PTE concentration in the stratum/PTE concentration of the baseline value; Table 1). The PLI values were characterized according to Tomlinson et al. (1980) (Table 2).

Foraminiferal analysis

Approximately 10 ml of sediment were prepared according to the protocol described by Murray (2006), which consists of separating the wet sediment fraction of interest, using a 63-µm sieve, to remove the excess of fine materials. Once the coarse

fraction of each sample is separated, it is oven-dried at a temperature < 50°C. Samples are then dry sieved (125 and 500 μm) to optimize the foraminiferal size-sorting, and the fractions are stored in properly identified containers, according to the horizon and sampled fraction. The sample was quartered and up to 300 specimens were obtained whenever possible. The specimens found in the sediment were screened and placed in foraminiferal holders. Specimens were identified whenever possible at species level following the taxonomic works not only of Loeblich Jr and Tappan (1964); Loeblich and Tappan (1988) but also of Debenay et al. (1998, 2001a), Semensatto-Jr and Dias-Brito (2004), Raposo et al. (2016), and Alves Martins et al. (2019b).

To assess foraminiferal change in the core, several indices were calculated:

- A. Species richness provides information on biodiversity: SR = number of individual species/sample.
- B. Shannon index estimates species diversity: $H' = -\sum pi \times lnpi$ (Shannon 1948). The higher the value, the greater the species diversity.
- C. Equitability assesses the evenness of the distribution (H'): $J' = H' / \ln S$ (Magurran 1988). Values range from 0 (uneven distribution) to 1 (even distribution).
- D. Foraminiferal density provides information on the abundance of foraminiferal specimens: FD = number of specimens/g of bulk sediment.
- E. The Ammonia/Elphidium Index provides information on sediment oxygenation levels: AEI = [NA / (NA + NE)] × 100 (Sen Gupta et al. 1996). Cribroelphidium species (e.g., C. poeyanum) have been classified as stress tolerant (Jorissen et al. 2018) and included in the calculations. The AEI values range from 0% (well oxygenated) to 100% (dysoxic–anoxic).
- F. The Foram Stress Index assesses the tolerance of species with respect to organic matter: $FSI = (10 \times Sen) + (Str)$ (Dimiza et al. 2016), where "Sen = sensitive" and "Str =

Table 2 Enrichment factor (EF) classification according to Sutherland (2000), sediment pollution index (SPI) classification according to Singh et al. (2002), and PLI values classified according to Tomlinson et al. (1980)

EF ranges	EF classification	SPI ranges	SPI classification	PLI values	PLI classification
EF < 2	Minimal enrichment. Suggests null or minimal contamination.	0–2	Natural sediments	0	Indicates natural conditions
2 < EF < 5	Moderate enrichment	2–5	Low polluted sediments	1	Indicates presence of PTE baseline levels
5 < EF < 20	Significant enrichment	5–10	Moderately polluted sediments	>1	Progressive deterioration
20 < EF < 40	Very high enrichment, indicating high level of contamination	10–20	Highly polluted sediments	_	_
EF > 40	Extremely high enrichment, indicating extreme contamination	> 20	Dangerous sediments	_	



- stress tolerant." The categories are as follows: 1.0–2.0 (heavily polluted), 2.0–5.5 (moderately polluted), 5.5–9.0 (slightly polluted), and 9.0–10.0 (normal/pristine). If values are zero, it represents azoic conditions.
- G. Unbiased entropy of diversity: EcoQS = exp(H'bc) (Bouchet et al. 2012). Range of values for transitional environments are based on Bouchet et al. (2018): > 15 ("excellent"), 11–15 ("good"), 7–11 ("moderate"), 3–7 ("bad"), and < 3 ("poor").

Multivariate statistical analysis

Selected abiotic and biotic variables were used for statistical analysis to better understand their relationship and facilitate the interpretation of the results. Before being submitted to statistical analysis, the data were $\log (x + 1)$ transformed. Principal component analysis (PCA) was performed using the Software Statistica® 12 resources. Spearman rank-order correlations were also determined with correlations considered significant at p < 0.050.

Results

¹⁴C dating and compositional and granulometric characteristics of the core SP8

The results of ¹⁴C dating performed on fragments of shells and wood collected in the sediment layers 36–38 cm, 100–102 cm, 132–134 cm, and 148–150 cm are shown in Table 3. All sedimentological data are reported in Appendix 2. The minimum, maximum, average, and standard deviation values of sedimentary fractions and other textural parameters of the core SP8 can be found in Table 4.

The sediment mean grain size (SMGS) varies between 22 μ m (mud) and 290 μ m (medium sand). The overall sediment grain size distribution varies from coarser sand in the lower section of the core (176–98 cm) to muddy very fine sand towards core top (106–0 cm) (Figs. 2 and 3).

 Table 3
 Radiocarbon ages for the analyzed levels in the SP8 core

In general, the sediments are poorly to very poorly sorted (Fig. 3). Between 176 and 98 cm sorting values (mean: 4.1 \pm 0.6 µm) tend to be relatively higher, while in the muddy sediments between 64 and 0 cm, the sorting values decreased slightly (mean: 3.5 ± 0.4 µm) indicative of better-sorted sediments (Fig. 3 and 4a). The sediments are bimodal which indicates different particle sizes as evidenced by the first (76 μm, very fine sand) from 95 to 0 cm and a second mode (605 μm, coarse sand) from 95 to 176 cm. In this upper section, very angular or angular particles predominate in the very fine sand fraction, whereas in the lower core section, the coarser sand fractions consisting of frosted patina sand grains of eolian provenance with shapes varying between very angular and rounded (Fig. 4). It is important to highlight that between 8 and 0 cm, the composition of the sediment particles in the fraction > 500 µm corresponds to plastic fragments (Fig. 4b).

Geochemical and mineralogical composition of the core SP8 sediments

The TOM values range from 0.1 to 7.6% (2.4 \pm 1.5%) with two peaks between 152 and 116 cm and from 44 to 0 cm (Table 4, Fig. 2). The CO₃ values vary from 1 to 11% (3.9 \pm 2.7%) (Table 4). The depth plot distributions of 18 elemental concentrations are shown in Fig. 2 and their ranges are presented in Table 4. The highest concentrations of Al (3.8 \pm $0.8\% \text{ mg kg}^{-1}$) and Cu (13.9 ± 7.1 mg kg⁻¹) are found between 176 and 70/80 cm depth and decrease at the core top, while Ca, Sr, Co, and Mn concentrations show a marked increasing trend from core base to top. Magnesium, Ni. Sc. Cr. and Ti have lower concentrations between 174 and 156 cm and higher and slightly variable between 156 and 0 cm. Arsenic has a similar pattern but shows a marked decrease in values between 50 and 40 cm depth. Zinc shows no changes in concentration from core base up to 40 cm followed by a rapid and marked concentration increase up to 433.7 mg kg⁻¹ at 24 cm, then subsequently slightly decreases towards the core top. A similar trend is observed for Cd, which also reaches the highest concentrations (2.1 mg kg⁻¹) at 24 cm. The concentrations of Pb and Hg are higher from the core base to about

Core	Layer (cm)	Sample	Conventional radiocarbon age years BP	Calibrated Age (2 SIGMA) years BP
SP8	38–36	Shell (bivalve)	1020 ± 170	1267 to 1207 (1237 ± 30)
	102–100	Shell (bivalve)	4890 ± 270	6182 to 6138 (6160 ± 22)
	134–132	Shell Fragments	7280 ± 410	9013 to 7310 (8162 ± 852)
	150–148	Wood	7530 ± 30	8330 to 8180 (8255 ± 75)



Table 4 Variation of granulometric parameters and chemical elements, total organic matter, and carbonate contents. Mean and standard deviation of each variable are also shown

Variables	Unity	Maximum	Minimum	Mean
Sediment mean grain size	μm	290	22	119 ± 77
Sorting	μm	5.09	2.79	3.85 ± 0.61
Skewness	μm	0.07	- 0.88	-0.35 ± 0.27
Kurtosis	μm	2.16	0.69	1.10 ± 0.37
Fine fraction (< 63 μm)	%	79.0	8.9	31.0 ± 14.8
Coarse sand (> 500 µm)	%	61.2	1.2	22.7 ± 18.3
Medium sand (500–250 μm)	%	25.4	0.3	11.1 ± 7.4
Fine sand (125–250 μm)	%	22.6	1.1	10.3 ± 5.9
Very fine sand (63–125 μm)	%	45.9	6.0	25.0 ± 11.6
Total organic matter	%	4.44	0.12	1.69 ± 1.13
CO_3	%	3.71	1.02	1.92 ± 0.79
Al	%	4.7	3.2	3.8 ± 0.8
As	${ m mg~kg}^{-1}$	9.9	1.8	7.0 ± 2.7
Ca	%	1.8	0.0	0.9 ± 0.6
Cd	${ m mg~kg}^{-1}$	2.1	0.1	0.5 ± 0.7
Co	${ m mg~kg}^{-1}$	10.5	2.2	7.8 ± 2.8
Cr	${ m mg~kg}^{-1}$	71.2	40.8	59.2 ± 13.9
Cu	${ m mg~kg}^{-1}$	27.6	7.0	13.9 ± 7.1
Hg	${ m mg~kg}^{-1}$	0.90	0.02	0.12 ± 0.21
Mg	${ m mg~kg}^{-1}$	1.46	0.24	1.11 ± 0.35
Mn	${ m mg~kg}^{-1}$	1036.0	63.0	521.2 ± 292.9
Mo	${ m mg~kg}^{-1}$	10.1	0.3	2.5 ± 2.4
Ni	${ m mg~kg}^{-1}$	22.8	7.7	18.1 ± 5.0
Pb	${ m mg~kg}^{-1}$	60.6	17.7	30.6 ± 14.2
Sc	${ m mg~kg}^{-1}$	8.8	4.1	7.4 ± 1.9
Sr	${ m mg~kg}^{-1}$	125.8	21.2	73.8 ± 26.7
Ti	%	0.06	0.02	0.05 ± 0.01
Zn	${ m mg~kg}^{-1}$	433.7	27.6	149.2 ± 131.0
U	${ m mg~kg}^{-1}$	6.2	1.8	3.5 ± 1.3

134 cm and 158 cm, respectively, followed by a decrease and subsequently increasing between 40 and 0 cm. Uranium and Mo show an increase in values from the core base up to 150 cm where they reach maximum concentrations (6.2 mg $\rm kg^{-1}$ and 10.1 mg $\rm kg^{-1}$, respectively), followed by a decreasing trend towards the core top. However, Mo reached a minimum at 40 cm followed by a slightly increasing trend between 40 and 0 cm, whereas U maintained relatively decreasing concentrations Appendix 2.

The mineralogical composition of the fine fraction is presented in Appendix 2. The most abundant minerals are phyllosilicates (59.5 \pm 12.6%), quartz (24.1 \pm 9.2%), plagioclase (5.3 \pm 5.8%), K-feldspar (2.1 \pm 3.7%) followed by calcite (2.2 \pm 2.3%), siderite (1.4 \pm 2.2), pyrite (1.0 \pm 1.2%), and anhydrite (0.6 \pm 1.9%) (Fig. 5). At some levels, the presence of opal C/CT, aragonite, hematite, anatase, magnetite/maghemite, and bassanite has also been identified. The

percentages of phyllosilicates, quartz, plagioclase, and K-feldspar are variable in the core but the depth plots do not show any clear changing pattern, except for plagioclase that is not found in the 176–160 cm interval (Appendix 3). The presence of pyrite is only identified between 140 and 10 cm (Fig. 5). Low percentages of hematite are also found at the base and core top. Calcite and feldspar/quartz values are minimal in the lower core section but tend to increase towards the core top. Anhydrite peaks are observed at the core base and also between 85 and 80 cm of depth.

PCA based on sedimentological data

The PCA based on elemental, mineralogical, TOM, and CO_3 data and particle size parameters show that the first two factors explain most of the data variability (total: $\sim 70\%$; factor 1: $\sim 50\%$; factor 2: $\sim 20\%$). The biplot of factor 1 against factor 2



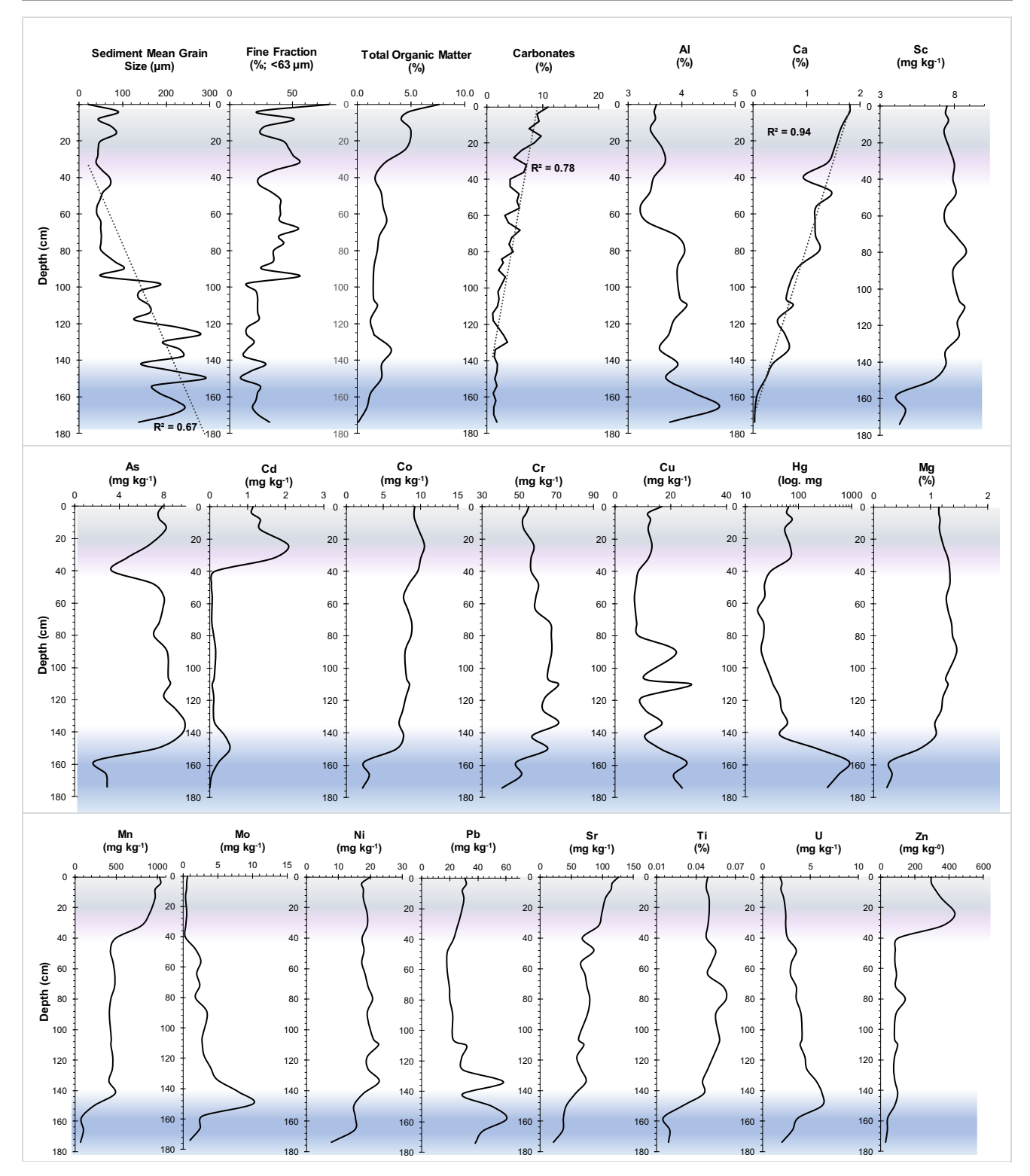


Fig. 2 Depth plots of sediment mean grain size and fine fraction, total organic matter, carbonate, and elemental contents. The regression line (dotted) and the respective \mathbb{R}^2 were represented in some graphs. The

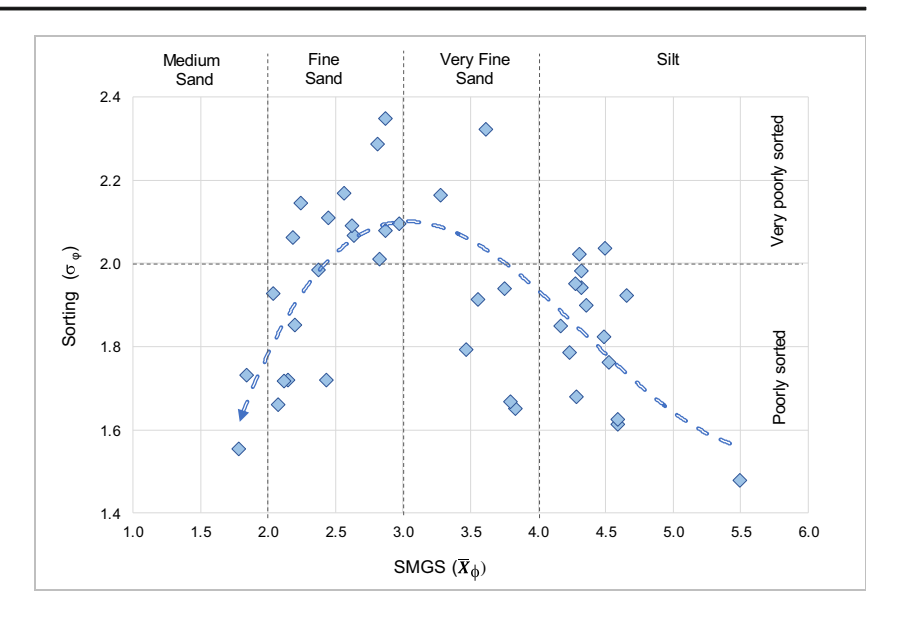
lower and the upper core sections were shaded to point out significant changes in several variables

(Fig. 6) reveals, for example, that As, Ni, Sc, Mg, Co, Ti, Mn, Sr, Ca, Zn, Cd, calcite, CO₃, TOM, and feldspar/quartz are related to finer-grained sediment (fine fraction, very fine sand

fraction, and fine sand fraction), whereas U, Mo, Al, Pb, Cu, Hg, anhydrite, and hematite contents are more associated with coarse-grained sediments (as indicated by SMGS, medium



Fig. 3 Phi-scale graph of the values of the sediment mean grain size (SMGS) against the sorting values. A trend line (dashed line) is represented (the values of 68 cm and 94 cm were excluded as outliers)



sand fraction, and coarse sand fraction). These results also show that Sc is more related to fine-grained sediments than Al. This supports the idea of using Sc as a normalizer in this core for the calculation of EF values. Although Al is widely used as a normalizer, in this case, the element/Sc ratio best minimizes the possible trend effects caused by the granulometry and allow identifying differences in the sediment composition not related to the sediment grain size (Loring 1988; Loring and Rantala 1992; Bueno et al. 2019). Scandium makes part of the structure of clay minerals and micas and so is a good indicator of the presence of these minerals particularly in sediments enriched in aluminosilicates (Dias and Prudêncio 2008), as evidenced by the analyzed mineralogical data of the study area. Most importantly, Sc is a very immobile trace element that makes it very resistant to weathering processes (e.g., diagenesis) (Zhao and Zheng 2015).

Enrichment factors

The EF values are presented in Table 5. The maximum EF values (> 2) are, in decreasing order, reached for Cd (23), Ca (14), Zn (8), Mn (7), Cu (5), Hg (4), Ti, Sr, Ni, Co, Mg (3), and Pb (2) (Fig. 7). The EF values of Al, As, Cr, Mo, and U do not increase above 1. The PLI and SPI values reach 3 and 23, respectively (Fig. 7). The EF-Cd, EF-Zn, EF-Mn, PLI, and SPI mostly increase in the upper 40 cm. The PLI values exhibit two increasing phases, one around 160 cm and the other from 40 cm depth. The SPI values have a similar pattern but have a reduced increase between 160 and 140 cm. The EF-Ca, EF-Sr, EF-Mn, and EF-Co have lower values at the core base and tend to increase towards the top. The EF-Cu reached the highest values at 158 cm and then subsequently decreasing up to 80 cm; from this layer, the values remain slightly variable up to the core top. The pattern of EF-Ni is similar to that of

EF-Cu. The EF-Hg and Sr/Ca values have a peak below 150 cm depth and present reduced and slightly variable values between 150 and 0 cm. The biplots and trend lines (and respective R^2 values) presented in Fig. 8 show positive correlations between the EF of several PTE pairs such as EF-Zn/EF-Cd, EF-Mn/EF-Cd, EF-Mn/EF-Ca, EF-Mn/EF-Co, EF-Mn/EF-Ca, and EF-Sr/EF-Ca.

Depth plots comparing the EF-Mo/EF-U ratio values (using Sc in shale as a normalizer) with Mn and Cd concentrations (Fig. 9a) and the biplot of EF-Mo versus EF-U values (Fig. 9b) show that samples between 174 and 150 cm experienced a noticeable enrichment in Mo concerning U followed by a depletion between 150 and 40 cm. All samples between 40 and 0 cm experienced a slight enrichment in Mo coupled with a significant increase in Mn and Cd.

Benthic foraminifera

No foraminifera are found in the interval between 176 cm and 136 cm (Fig. 10; Appendix 4). Less than 100 foraminiferal specimens occur at levels 130 cm and 110 cm (Appendix 4). Poorly preserved specimens (i.e., broken, dissolved) are documented in some layers and reduced in size (\leq 125 μ m) in the first 22 cm.

In total, 8813 specimens were collected in the studied layers, corresponding to 78 species/taxa of foraminifera (Appendix 4). The FD was < 5791, SR was < 28, J' was < 0.8, and H' was < 2.4 (Appendix 4). The depth plots presented in Fig. 10 show the barren samples between 177 and 140 cm depth. From 140 to 0 cm, the presence of foraminiferal tests becomes significant. Species richness, J' and H' values show a similar increasing/decreasing pattern (Fig. 10). The dominant foraminiferal genera between 136 and 0 cm are Elphidium, Cribroelphidium, and Ammonia genera (Appendix 4).



Fig. 4 a The predominant presence of very angular or angular particles in the composition of the very fine sand fraction. b The occurrence of microplastics in the fraction > 500 μm of the first 6 cm of the SP8 core. c Details of the fraction 125 to 500 μm, from the horizon 52 to 54 cm. d Details of the sandy fraction of the mesh 150 to 250 μm from the horizon 162 to 164. e, f Details of the fraction > 500 μm, from the horizon 150 to 152 cm and 162 to 164 cm



The dominant genera are *Elphidium/Cribroelphidium* and *Ammonia* genera (Appendix 4). The species with relative abundance $\geq 5\%$ are *Cribroelphidium poeyanum* (< 88.2%; 41.1 ± 25.9%), *Ammonia tepida* (< 75.9%; 16.0 ± 22.7%), *Buliminella elegantissima* (< 28.9%; 5.4 ± 7.7%), *Ammonia rolshauseni* (< 27.5%; 3.5 ± 5.8%), *Pararotalia cananeiaensis* (< 21.5%; 4.1 ± 5.9%), *Cribroelphidium excavatum* (< 19.6%; 6.6 ± 4.5%), *Bolivina fragilis* (< 16.9%; mean 0.6 ± 2.9%; with a peak at 48 cm; absent or rare in the other core layers), *Elphidium oceanense* (< 15.9%; 2.7 ± 4.0%), *Elphidium incertum* (< 15.8%; 3.5 ± 4.3%), *Elphidium advenum* (< 11.1%; 2.2 ± 3.0%), and *Porosononion granosum* (< 10.8%; 1.7 ± 2.9%), *Ammonia parkinsoniana* (< 6.7%; 3.2 ± 1.8%), *Bolivina*

striatula (< 6.5%; $1.4 \pm 1.9\%$), Bulimina aculeata (< 4.8%; $1.1 \pm 1.3\%$), and Elphidium discoidale (< 4.7%; $0.8 \pm 1.2\%$) (Figs. 11 and 12; Appendix 4).

Figure 11 illustrates some species found in core SP8 and Fig. 12 shows the depth plots of the relative abundances of the most abundant and frequent species. The graphs show, for instance, that *A. tepida* and *A. rolshauseni* are less abundant in the lower core interval, where foraminiferal assemblages are mainly composed of *Cribroelphidium* and *Elphidium* species (e.g., *C. poeyanum*, *C. excavatum*, *E. oceanense*, *E. incertum*, and *E. advenum*) but also include *P. granosum*, *B. aculeata*, and *Buccella peruviana*. *Pararotalia cananeiaensis* is rare in the lower core section, has a peak between 44 and 36 cm, and declines towards the core top.



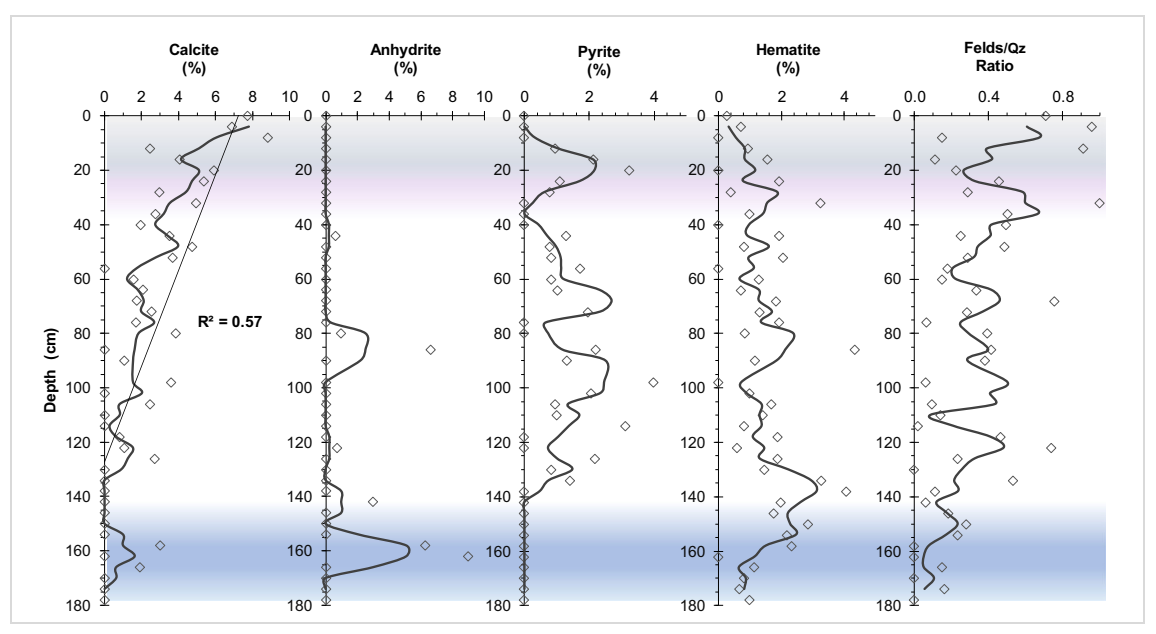


Fig. 5 Depth plots of calcite, anhydrite, pyrite, hematite percentages, and feldspars/quartz values. The regression line (dotted) and the respective R^2 were represented for calcite. The lower and upper core sections were shaded to point out significant changes in several variables

Buliminella elegantissima and B. striatula are mostly present in the upper 80 cm but the former declines in percentage between 32 and 0 cm.

In the section between 40 and 0 cm, there is a significant increase in the *Ammonia/Elphidium* Index ratio, towards the core top (Fig. 10). Trends in FSI, Exp(H'bc), and *J'* are quite similar. The FSI values range from 1 to 5.1 (Fig. 10; Appendix 4). Based on the FSI, "moderately polluted" conditions can be inferred from the core base to 56 cm that turn upwards to

"heavily polluted." The Exp(H'bc) values show an overall increasing trend from 134 to 40 cm, then decline in the upper part of the core. The highest values (12.3) of Exp(H'bc) have been found at 72 cm (Fig. 10).

PCA based on sedimentological and biotic data

The relative abundance of the main benthic foraminiferal species has been compared with selected sedimentological data

Fig. 6 PCA graph based on selected grain size and geochemical and mineralogical variables. Legend: SMGS, sediment mean grain size; sand, total sand fraction; MSF, medium sand fraction; CSF, coarse sand fraction; FF, fine fraction; FSF, fine sand fraction; VFSF, very fine sand fraction; TOM, total organic matter; Carb, carbonates; Hem, hematite, Anhy, anhydrite; Fds/Qz, feldspar/quartz ratio; Calc, calcite

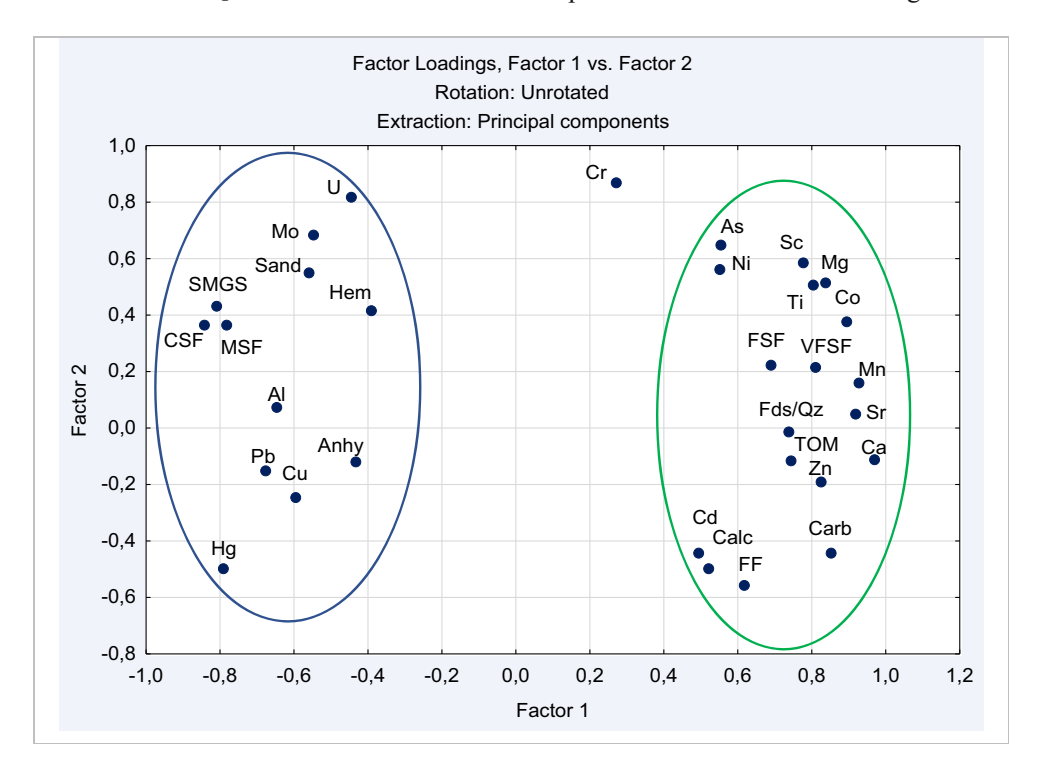




Table 5 Values of EF for the analyzed chemical elements (using Sc as normalizer) throughout the SP8 core. Values > 2 are marked. (*) - Mo and U only, the Sc background values used were from shale as described by Turekian and Wedepohl (1961)

					EF: 2	2-5;		EF: 5	-20;		EF: 2	0-40					
Depth (cm)	As	Cd	Со	Cr	Cu	Hg	Ni	Pb	Zn	Al	Ca	Mg	Mn	Мо	Sr	Ti	U
0	1	13	3	1	2	0	2	0	5	1	14	2	6	0	3	3	0
4	1	13	3	1	1	0	2	1	5	1	14	2	7	0	3	3	0
8	1	15	3	1	1	0	2	0	6	1	13	2	6	0	3	3	0
14	1	16	3	1	1	0	2	0	7	1	13	2	6	0	3	3	0
24	1	23	3	1	1	0	2	0	8	1	11	2	5	0	2	3	0
32	1	18	3	1	1	0	2	0	6	1	10	2	5	0	2	3	0
40	0	2	3	1	1	0	2	0	2	1	7	2	3	0	2	3	0
48	1	1	2	1	1	0	2	0	1	1	11	2	2	0	2	3	0
56	1	1	2	1	1	0	2	0	2	1	9	3	3	0	2	3	0
64	1	1	2	1	1	0	2	0	2	1	9	3	3	0	2	3	0
72	1	1	2	1	1	0	2	0	1	1	8	2	3	0	2	3	0
80	1	1	2	1	1	0	2	0	2	1	8	2	2	0	2	3	0
90	1	2	2	1	2	0	2	0	2	1	6	3	2	0	2	3	0
106	1	1	2	1	1	0	2	0	1	1	4	2	2	0	1	3	0
110	1	1	2	1	2	0	2	0	2	1	5	2	2	0	2	3	0
118	1	1	2	1	1	0	2	0	1	1	3	2	3	0	1	3	0
126	1	1	2	1	1	0	2	0	1	1	4	2	3	0	1	3	0
134	1	2	2	1	2	0	3	1	2	1	5	2	3	1	2	3	1
142	1	5	2	1	1	0	2	0	2	1	3	2	3	1	1	3	1
150	1	7	2	1	2	1	2	1	2	1	2	2	2	1	1	2	1
158	0	5	1	1	5	4	3	2	1	1	1	1	1	1	2	2	1
166	1	1	1	1	3	2	3	1	1	1	0	1	1	0	1	2	1
174	1	0	1	1	4	2	1	1	1	1	0	1	1	0	1	2	0

(granulometric, mineralogical, and geochemical parameters) by PCA. The first two factors explain ~ 69\% of the data variability (factor 1: $\sim 45\%$; factor 2: $\sim 23\%$). Based on the PCA results (Fig. 13) coupled to factor loadings (Appendix 5), it has been possible to infer: (1) SMGS, EF-Cu, EF-Hg, and anhydrite are positively related to factor 1; (2) EF-Ca, EF-Co, EF-Mn, EF-Sr, EF-Zn, CO₃, fines, feldspars/quartz, TOM, SR, J', H', FD, and the species A. tepida, A. parkinsoniana, A. rolshauseni, B. elegantissima, B. striatula, C. excavatum, C. gunteri, P. cananeiaensis, and P. japonica are negatively related to factor 1; (3) B. aculeata, E. incertum, E. advenum, E. oceanense, E. discoidale, A. parkinsoniana, C. excavatum, C. poeyanum, P. granosum, B. peruviana, SR, J', H', and FD are associated with positive values of factor 2; and (4) EF-Cd, EF-Zn, B. striatula, and TOM are negatively related to factor 2 (Fig. 13). The two first score factors of the PCA were plotted and compared with foraminiferal density, H', Ammonia/ Elphidium, FSI, SPI, and EF-Mo/EF-U values in Fig. 14. This figure allows us to integrate the most significant data of the core SP8 and to provide a general pattern of the temporal evolution of the study area (discussed in the next section).

Discussion

Age model and calibration

The pattern of Zn and Cd concentrations and the enrichment factors of these PTEs (Figs. 2 and 7) in the upper part of core SP8 is similar to other records studied for instance by Gomes et al. (2009) in three sediment cores sampled in Sepetiba Bay near the Guandu River mouth; Marques Jr. et al. (2006) in a

core collected in the Coroa Grande mangrove, located in the vicinity of Ilha da Madeira plant (Fig. 1); and Araújo et al. (2017a, 2017b) in cores T1–T5 collected in different locations of Sepetiba Bay. Based on these studies, we can estimate that the first 35 cm of core SP8 records the period after ≈ 1975 (Anno Domini; Figs. 2, 7, and 14), taking into account the beginning of cadmium production by the zinc smelter (Companhia Siderúrgica Ingá Mercantil) in 1974 (Rodrigues et al. 2020) and the maximum metal concentration in sediments at the 1980s (Patchineelam et al. 2011).

Considering the available radiocarbon data of ≈ 1.2 ka BP obtained for the layer 38–36 cm, it can be deduced that there was a significant loss of the sedimentary record, probably > 1000 years in the core SP8. This sedimentary discontinuity (SD) is marked in Fig. 14. The age model shown in Fig. 15 for the sedimentary column below 38 cm depth allows inferring a sediment accumulation rate of 1.3–2.4 cm for 100 years and to date with ≈ 9.5 ka BP the core base. As no evidence of bioturbation was observed in this core (most of it was deposited under suboxic conditions), it can be deduced that the estimated age model is coherent. Thus, the core SP8 is a siliciclastic upward-fining sequence that records most of the Holocene evolution of the study area.

Sedimentary environment between pprox 9.5 and 7.8 ka BP

The lower section (170–140 cm) of core SP8 has coarser-grained sediments deposited between ≈ 9.5 and 7.8 ka BP. Sediments of this lower section, have low CO₃, calcite, and hematite contents as well as feldspar/quartz and EF values of several elements (i.e., Ca, Co, Mg, As, Mn, and Ti). Pyrite is



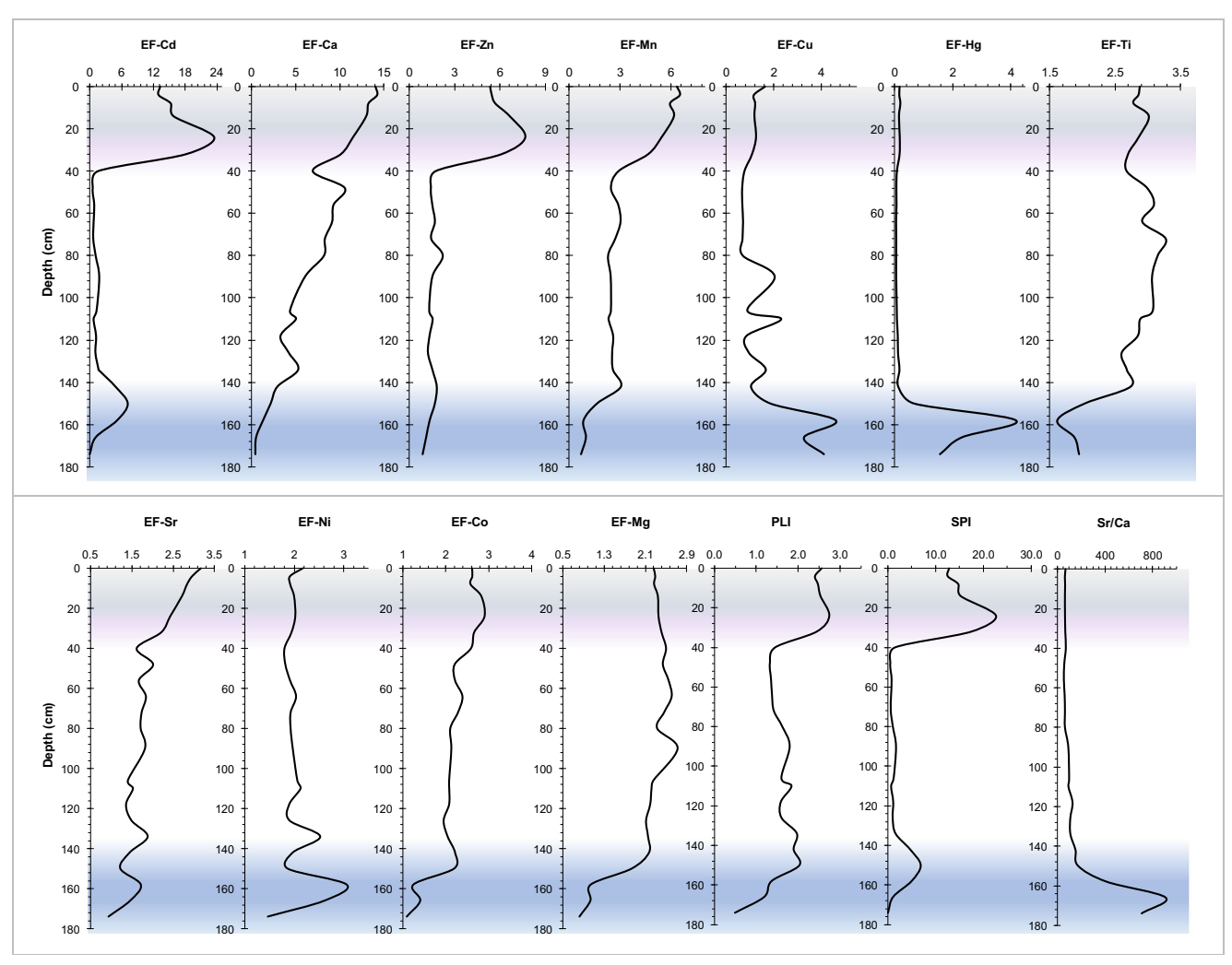


Fig. 7 Depth plots of enrichment factors (EFs) of elements that reach minimum values >2. The depth plots of the PLI, SPI and Sr/Ca values are also shown. The lower and upper core sections were shaded to point out significant changes in several variables

not found in these layers, since the low amount of TOM did not favor the formation of this mineral (Aberner 1984). This dataset denotes the presence of a mineralogical component different from that found in the upper layers and also the presence of a dissimilar sedimentary environment. The absence of foraminiferal and mollusk remains, also, to high Sr/ Ca values towards the bottom of the core, the low values of Ca-Mg, CO₃, feldspar/quartz, and Ti/Al values (proxy of eolian processes; Chen et al. 2013) coupled with higher values of Al (proxy of terrestrial input; Larson et al. 2015) and hematite suggest the occurrence of subaerial environments. The relatively high abundance of coarse sand particles wind-shaped (rounded frosted patina grains of quartz) allow supposing that wind was an important transport agent in this region. Indeed, it can be inferred that these sediments were likely deposited under subaerial and dryness conditions associated with eolian processes and strong winds.

A study by Borges and Nittrouer (2015) described subaerial environments and identified river paleoenvironments

during a sea-level lowstand in the late Pleistocene. A sinuous paleo-channel located towards the southern margin of the bay, ran parallel close to today's Marambaia barrier island and exiting towards the west of the bay corresponding to Marambaia Island (topographic high) and where core SP8 was collected. High-resolution seismic stratigraphy also supports the presence of fluvial channels and sedimentary deposits (Reis et al. 2020). Thus, the sedimentary units between 178 and 140 cm are interpreted as being deposited in a fluvioterrestrial environment close to a high-energy sandy coast during a period of lower sea level (Angulo and Lessa 1997; Castro et al. 2014; Jesus et al. 2017). Also, it is speculated that short-lived marine incursions or wash over deposit events (Hayes 1967; Coates 1973) potentially creating brine-ponds could have allowed for the precipitation of non-biogenic calcite and anhydrite evaporitic minerals (Sinha and Raymahashay 2004).

These marine incursions were detected in the Juréia region, situated in the southeast coastal area of Brazil. A detailed



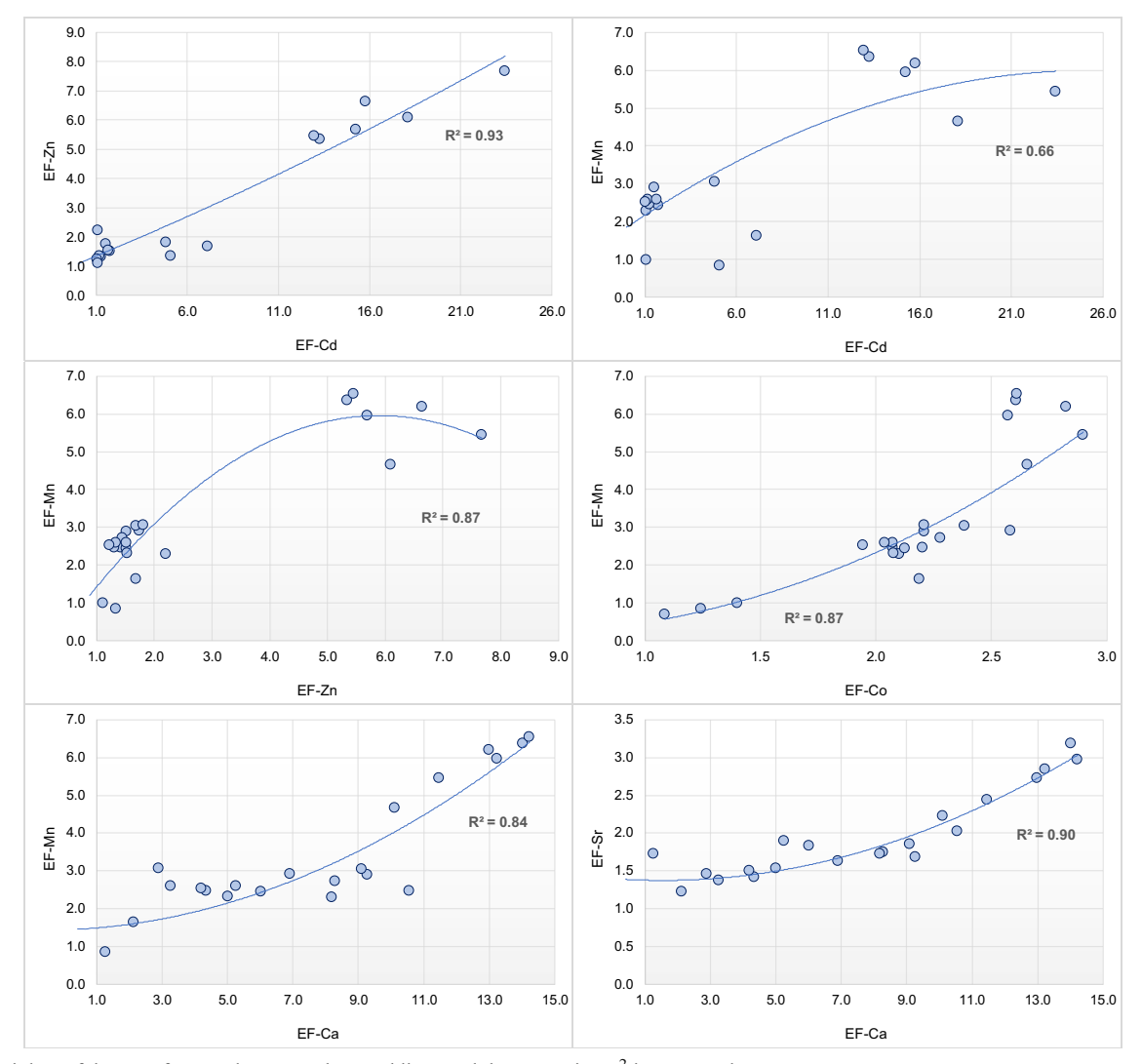


Fig. 8 Biplots of the EF of some elements. The trend lines and the respective R^2 is presented

paleoclimatic record of Juréia Paleolagoon indicates that in about 9400 cal year BP, a lagoon environment was established, with mixed continental and marine contribution, favoring benthic foraminifera (Sallun et al. 2012; Silva et al. 2014). According to Silva et al. (2014), there were four phases of conspicuous marine incursions (i.e., 9400–9338 cal year BP, 9075–8894 cal year BP, and 8541–8500 cal year BP) intercalated with two phases of prominent continental contribution (9338–9072 cal year BP and 8500–8385 cal year BP). The change in dominance from continental sources was indicated by lead isotopes, which indicated stability in sea level and also increase in rainfall and sediment inflow in Juréia (Sallun et al. 2012).

During the interval, ≈ 9.5 –7.8 ka BP, the records of core SP8 indicate that the sediment source consisted of reworked mature lithics from nearby drainage basins (at that time, several river mouths were located near the study area, according to Reis et al. 2020) and from nearby rock outcrops probably of the Marambaia Massif (Fig. 1c). The elemental

composition and concentration of the sediments depend on the source rock (Arunakumara et al. 2013; Ali et al. 2019) as these geological materials may have high concentrations of such elements (e.g., Cr, Co, Ni, Cu, Zn, Cd) (Turekian and Wedepohl 1961; Wedepohl 1995). For instance, igneous rocks composed of olivine, hornblende, and augite provide the sediment background values for Co, Ni, and Zn among others (e.g., Martínez-Colón et al. 2009; Ramakrishna and Gill 2019). Excessive weathering (e.g., leaching) could explain the ephemeral natural background enrichment spikes of Cd, Cu, Co, and Ni as evidenced by high SPI values (Figs. 7 and 14).

A conspicuous enrichment of Mo with respect to U is observed around 8.25 ka BP (150 cm; Fig. 9a, b), a change that has been interpreted as an indicator of an environmental transition to anoxic conditions (e.g., Algeo and Tribovillard 2009; Lu et al. 2011; Rico et al. 2019). Under such conditions, redox-sensitive PTEs would be scavenged from the water column, resulting in increased concentrations of Pb, Hg, Mo, U



Fig. 9 a Depth plots comparing the EF-Mo/EF-U ratio values with Mn and Cd concentrations. b Biplot of EF-Mo versus EF-U values. Both graphs show changes in the sedimentary environment. Single arrowheads indicate direction of environmental change in relation to core sample depth. Rectangle highlights the clustering of samples associated with anthropogenic influence. Taken and modified from Algeo and Tribovillard (2009)

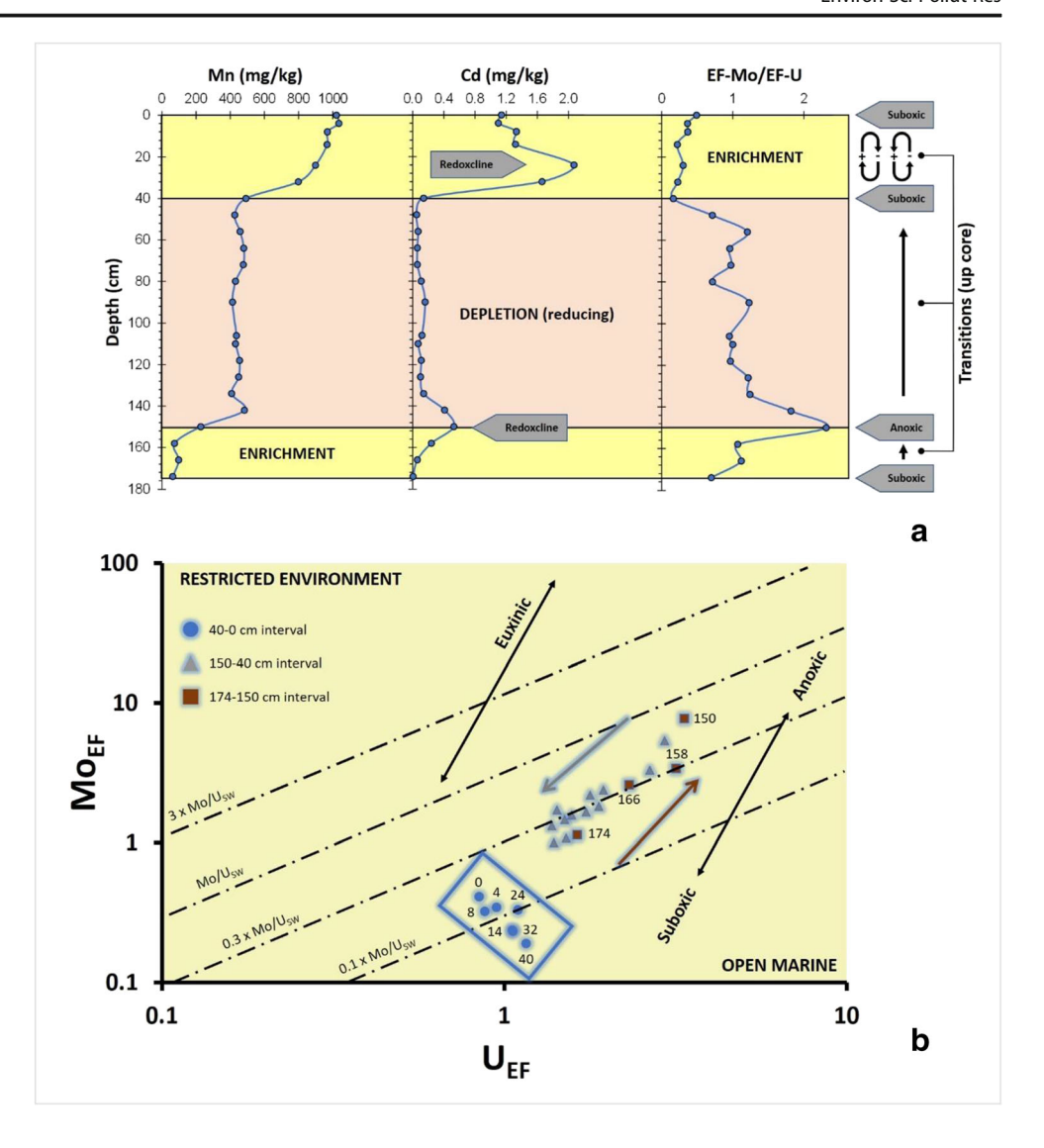


(Fig. 2), and higher EF values (for instance Cd, Cu, Hg, Ni, Mo, U; Fig. 7). This period is also marked by increased concentrations of TOM, possibly driven by the same conditions recorded in the Juréia coastal region between 8300 and 8210 cal year BP (Sallun et al. 2012). During this time, the rapid acceleration of ice melting in North America slowed the Atlantic Meridional Overturning Circulation, causing an abrupt cooling of 1-3 °C in large parts of the Northern Hemisphere (Thomas et al. 2007; Schmidt and LeGrande 2005; Morrill et al. 2013; Matero et al. 2017). In the Southern Hemisphere, the South American Summer Monsoon was intensified in Brazil (Cheng et al. 2009), resulting in increased rainfall and moisture (Sallun et al. 2012). Unfortunately, our data do not allow further investigations about the source of the organic matter. Nonetheless, considering that the sedimentation of this period was mostly continental, in a transitional fluvio-marine environment, it can be hypothesized that terrestrial plants were the source of the organic matter, probably mangrove forests similar to those

currently found in the Guaratiba coastal plain (Fig. 1a, b). SPI values attest to the increased sediment toxicity that reached levels of "moderately polluted sediments" (Singh et al. 2002; Table 2, Fig. 14), solely related to natural processes. According to Sallun et al. (2012), a second anomalous period occurred between 8200 and 8000 cal year BP, characterized by rapidly decreasing sediment accumulation rates in the Juréia coastal plain. In the study area, this second anomaly is marked by a significant change in the sediment composition (Figs. 2, 4, and 14), signed by the decreased values in the variables that marked the previous event.

Regarding yet drivers of metals retention in the sediments, in the case of As, its natural background concentrations as revealed by the EF (up to 1) are low (Fig. 2) between 9.3 and 8.7 ka BP (174–160 cm) and around 1.4 ka BP (40 cm), and its variability is tied to the ever-changing reducing conditions of the bay throughout its history. As mentioned by Magalhães and Pfeiffer (1995) and Martínez-Colón et al. (2009), As⁺⁵ and As⁺³ will be bound to oxide–hydroxides



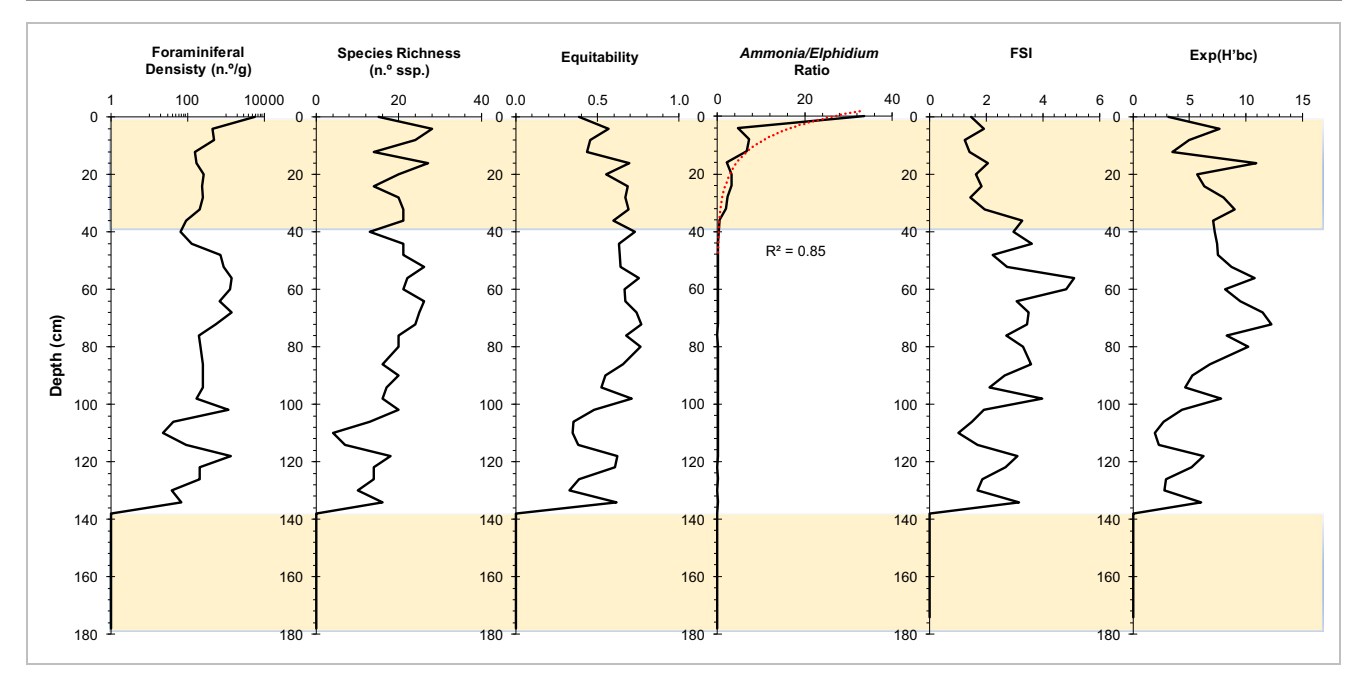


Fig. 10 Depth plots of the values of foraminiferal density, species richness, equitability, the Ammonia/Elphidium ratio, FSI, and Exp(H'bc) values along the SP8 core. The logarithmic regression line and the respective R^2 was represented in Ammonia/Elphidium graph.

The upper core section where the values of the *Ammonia/Elphidium* ratio increase significantly was shaded, as well as the lower one without foraminifera

(oxic) or sulfides (anoxic), respectively, and this is evidenced by the noticeable changes of As concentrations in the sediments deposited between ≈ 8.7 and 1.4 ka BP (section 160-40 cm). Several studies from cores and surface sediment samples from Sepetiba Bay have reported As, as being anthropogenic in origin due to metallurgic effluents (Araújo et al. 2017a, 2017b; Díaz Morales et al. 2019). The observed concentrations at least in the study area support the idea that the As contributions are mostly related to natural sources associated with the weathering of source rocks from the region.

Marine–estuarine sedimentary environment (pprox 7.8–1.2 ka BP)

The sediments between 140 and 40 cm are characterized by a noticeable increase in relatively poorly sorted muddy fine sands. At the lower part of this section $(140 \text{ cm}) \approx 7.8 \text{ ka}$ BP, it is inferred that the Marambaia Cove was flooded during a marine transgression as observed by a transition from fluvioterrestrial to marine conditions. At the beginning of the Holocene, the mouths of the rivers were located close to the study area (Reis et al. 2020). With the sea-level rise, they were progressively more distant (migrating to N for the current position); this process triggered a decrease in the phyllosilicates supply to the study area, as indicated by the progressive reduction of Al towards the core top (Fig. 2). Friederichs et al. (2013) and Borges and Nittrouer (2015) estimated the age of the maximum flooding surface (MFS) mapped inside Sepetiba Bay to be ~ 6.0 –5.8 ka BP. Our

results support this environmental transition based on the significantly lower Sr/Ca ratios, coupled with increased carbonates and biogenic calcite found in the sediments, and also by the first appearance of the benthic foraminifera Pararotalia cananeiaensis (Debenay et al. 2001a) among other calcareous organisms, such as other foraminifera species and mollusks. However, the newly established conditions were not open marine. The amount of TOM within this section increased significantly indicative of variable redox conditions which coincide with a persistent degree of environmental confinement and limited circulation (Fig. 14). The supply of organic matter favored the establishment of sedimentary suboxic conditions as indicated by the Mn values and the EF-Mo/EF-U ratio (Figs. 2, 9). Although the overall conditions of the lagoon evolved from anoxic to a suboxic environment (depletion of Mo with respect to U), it is hypothesized that the presence and variable abundance of pyrite (0–2.8%) found in the sediment fine fraction formed under anoxic microenvironments (e.g., pore spaces, sediment-water interface). Such chemical transition has further implications on the fate and transport of PTEs. Under suboxic conditions, PTEs will be re-released into the water column and potentially sequestered or adsorbed into other phases (e.g., bound to clays).

The sediments in this section are not polluted by PTEs based on the low PLI and SPI values and by the overall low EF (< 2) of Cd, Zn, Hg, Ni, and Cd, and although Díaz Morales et al. (2019) reported the highest concentrations (exceeding Brazilian legislation) of these PTEs in a sampling station (S30) near core SP8, our study found that only Pb



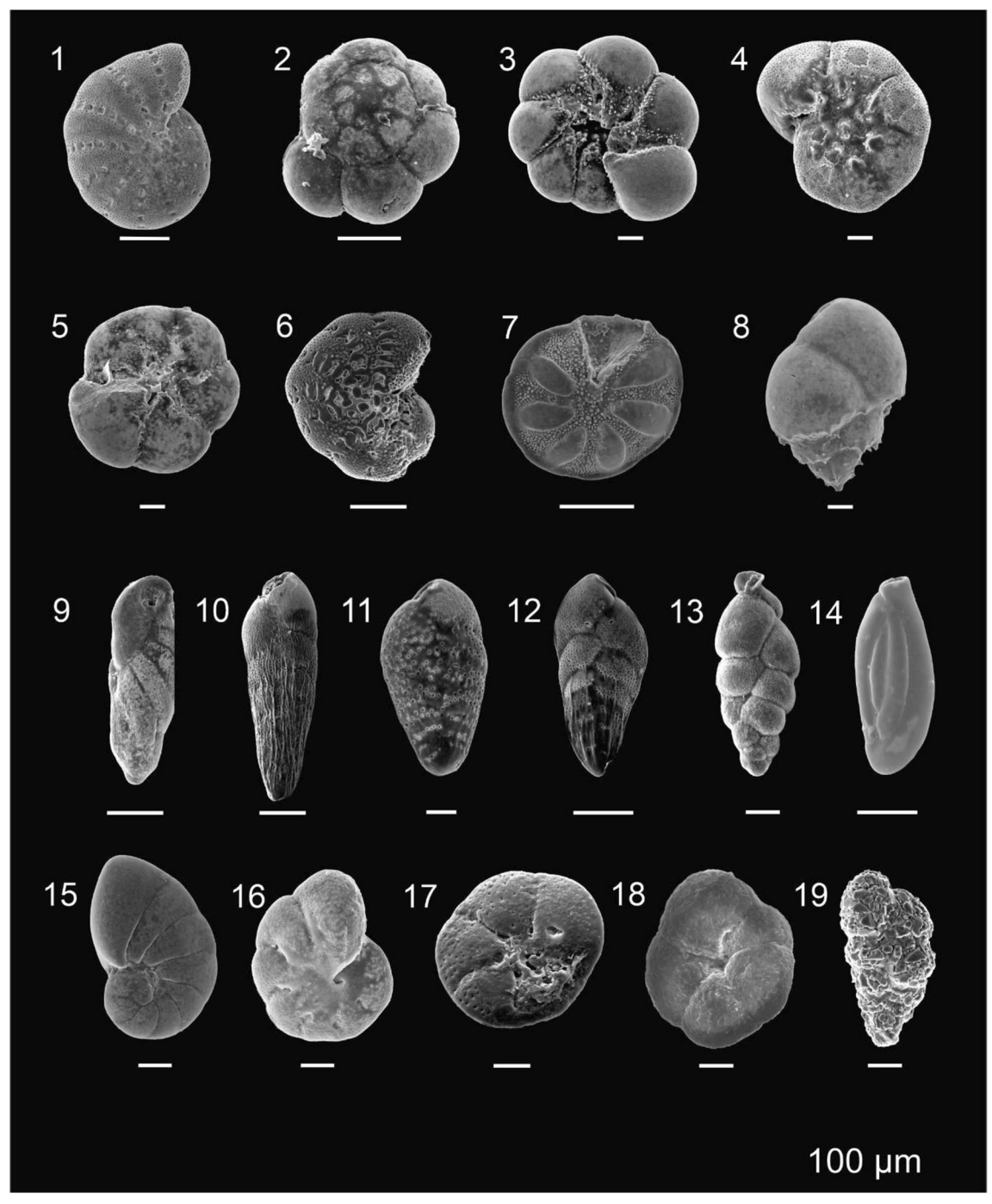


Fig. 11 Scanning electron microscopy images of selected foraminiferal species identified along the SP8 core. (1) *C. poyanum*. (2) *A. tepida*. (3) *A. tepida*. (4) *A. parkinsoniana*. (5) *A. rolshauseni*. (6) *C. excavatum*. (7) *B. peruviana*. (8) *B. aculeata*. (9) *B. elegantissina*. (10) *B. striatula*. (11)

B. compacta. (12) B. fragilis. (13) H. pacifica. (14) Q. laevigata. (15) P. japonicum. (16) A. gallowayi. (17) R. auberii. (18) C. exilis. (19) R. squamiformis

has consistently exceeded naturally those values (> 20 mg kg⁻¹) (Fig. 2). The background moderate enrichment of Co is related to the conditions of the lagoon. The positive correlation between EF-Co and EF-Mn (Fig. 8) suggests that Co is intimately related to the processes of Mn retention in sediments, that is, with the formation of Mn oxy-hydroxides given that Co geochemically resembles Fe and is found

coprecipitated and adsorbed into manganese oxides (Hem 1985).

The values of the feldspar/quartz ratio are quite variable in this section but tend to be higher than in the previous one, indicative of accumulation of sediments from several sources and less reworked by coastal processes. For example, the PCA - factor score 1 (Fig. 14) indicates that the Marambaia



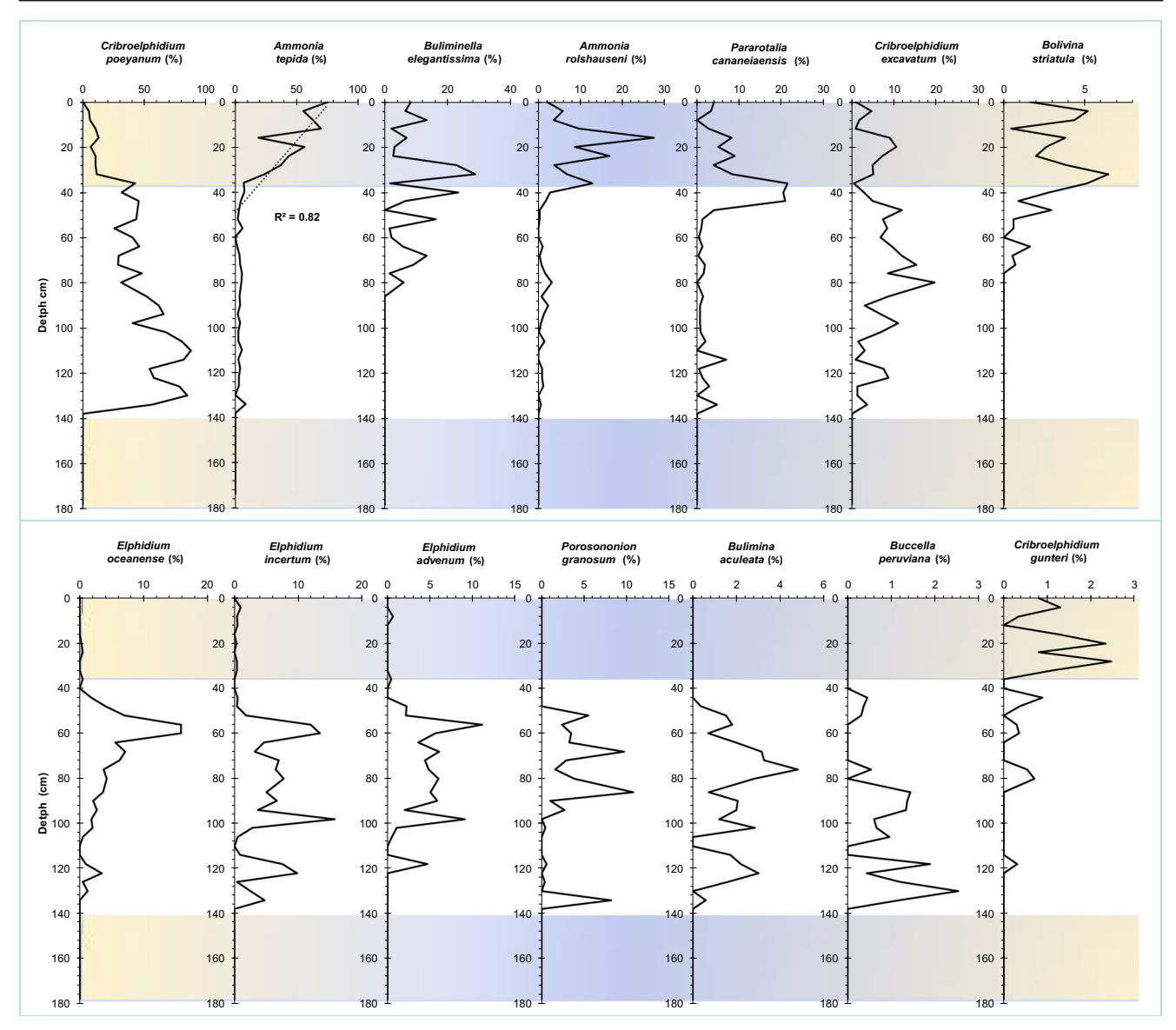


Fig. 12 Depth plots of the percentage of the most abundant benthic foraminiferal species in the SP8 core. The regression line and respective R^2 for *A. tepida* was represented. The upper core section where the

relative abundance of this species increases was shaded, as well as the lower one without foraminifera

Cove became progressively confined after ≈ 7.8 ka BP, related to the formation and evolution of the Marambaia barrier island (Friederichs et al. 2013). This confinement or environmental encroachment helps in the retention of sediments (e.g., organic matter) from proximal (coastal drift) and distal (river supply) sources. These data summarized in the depth plot of the PCA - factor score 1 (Fig. 14) indicate that the Marambaia Cove became progressively confined after ≈ 7.8 ka BP, as the Marambaia barrier island developed (Friederichs et al. 2013).

Given the newly established marine conditions, the foraminiferal assemblage in this section is dominated by the oxygensensitive elphidiids, mostly *C. poeyanum* associated with not only *C. excavatum*, *E. oceanense*, *E. incertum*, *E. advenum*,

and *E. discoidale* but also *P. granosum*. They also included other species such as *B. aculeata*, *B. peruviana*, and *A. tepida* in very low abundances (Fig. 12). This assemblage, which is quite common in Brazilian transitional environments (e.g., Laut et al. 2016; Pinto et al. 2016; Duleba et al. 2018), typically controls the dominance and distribution of foraminifera as supported by their positive correlation with FD, SR, *H'* and *J'* (PCA group III; Fig. 13). Also, the mean *H'* values (1.7) are typical of a shallow marine transitional environment as reported by numerous authors in other estuarine environments from Puerto Rico (Martínez-Colón and Hallock 2010; Martínez-Colón et al. 2017, 2018), Brazil (e.g., Pregnolato et al. 2018), and Italy (e.g., Armynot du Chatelet et al. 2016) among others. The values of PCA factor 2, positively correlated with



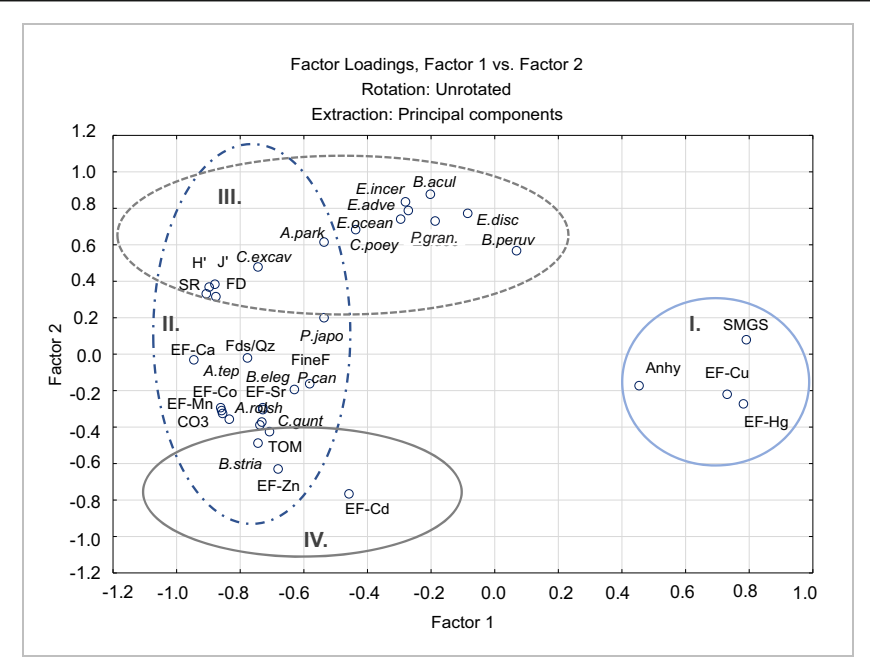


Fig. 13 Graph of factor 1 against factor 2 of the principal component analysis (PCA) based on selected data (granulometric, geochemical and biotic). Sets of variables that are more positive and negatively related to each of these factors are highlighted. Caption: *C.poey*, *Cribroelphidium poeyanum*; *A.tep*, *Ammonia tepida*; *B.eleg*, *Buliminella elegantissima*; *A.rolsh*, *Ammonia rolshauseni*; *P.can*, *Pararotalia cananeiaensis*; *C.excav*, *Cribroelphidium excavatum*; *E.ocean*, *Elphidium oceanense*; *E.incer*, *Elphidium incertum*; *E.adve*, *Elphidium advenum*; *P.gran*.,

P. granosum; A.park, Ammonia parkinsoniana; B.stria, Bolivina striatula; E.disc, Elphidium discoidale; B.acul, Bulimina aculeata; P.japo, Pseudononion japonicum; B.peruv, Buccella peruviana; C.gunt, Cribroelphidium gunteri; SR, species richness; H', Shannon index; J', equitability; FD, foraminifera density; Fines, fine fraction; TOM, total organic matter; CO₃, carbonates; SMGS, sediment mean grain size; Anhy, anhydrite

higher FD, H', and J' (namely with the presence of B. aculeata, E. incertum, E. advenum, E. oceanense, Elphidium discoidale, A. parkinsoniana, C. excavatum, C. poeyanum, P. granosum, and B. peruviana) are indicative

of relatively favorable conditions. The Exp(H'bc) values (Fig. 10) show an overall progressive improvement during this time interval from "poor" to "good" environmental conditions as well as with the FSI (Fig. 10) showing a change from "heavily

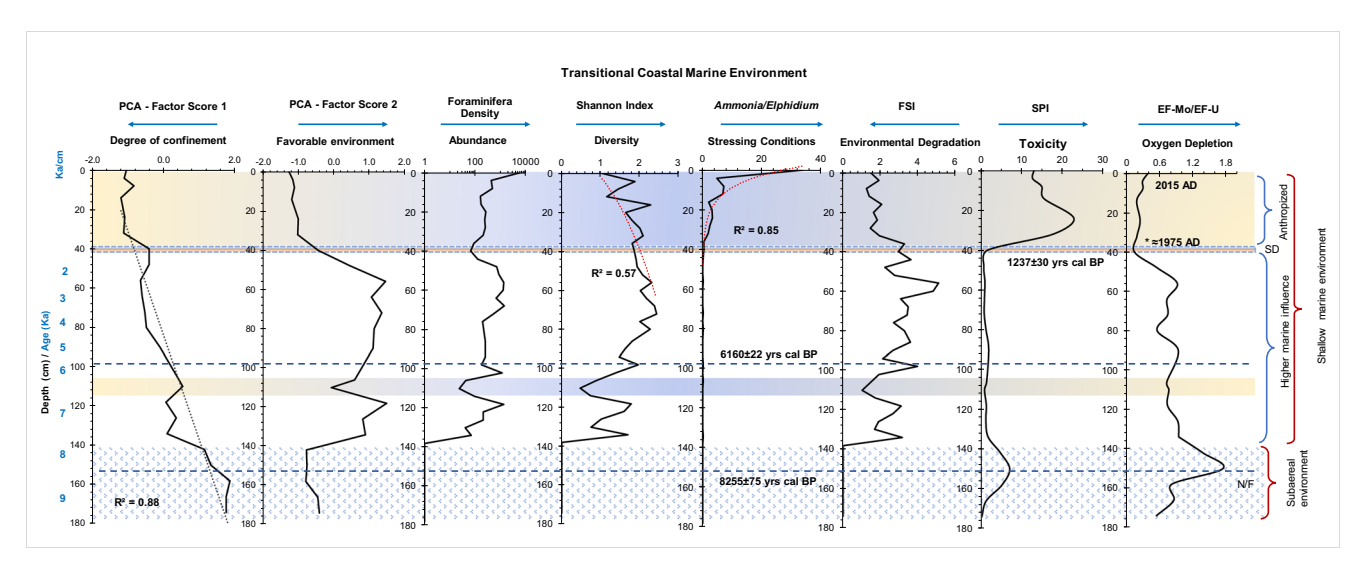
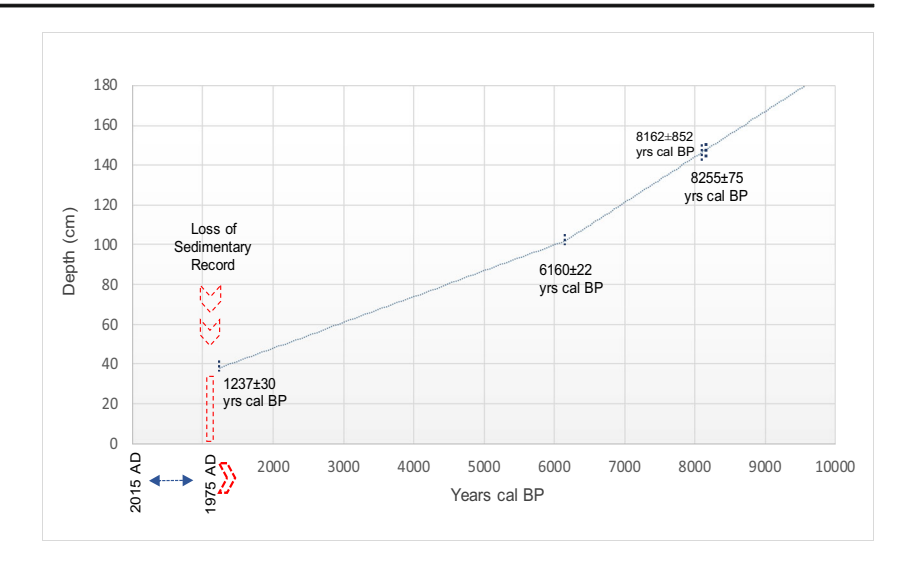


Fig. 14 Comparison of the two first score factors of the PCA of Fig. 13 with foraminifera density (n.°/g), Shannon index, *Ammonia/Elphidium*, FSI, SPI, and EF-Mo/EF-U values. Dated levels by 14C are identified associated with a sedimentary discontinuity around \approx 38 cm depth with the estimated age (*) from Castelo et al. (submitted). The regression lines and the respective R^2 are represented for the PCA score factor 1 are

represented for: the upper 86 cm of Shannon index values and the upper 40 cm of *Ammonia/Elphidium* Index values. Some events were highlighted based on the interpretation of the SP8 core data. Legend: SD, sedimentary discontinuity; N/F, barren foraminifera; AD, Anno Domini; yrs, years; cal, calibrated; BP, before present



Fig. 15 SP8 core age model, established by interpolating the radiocarbon ages and other sedimentary records (see the discussion in the text). Legend: AD, Anno Domini



polluted" to "moderately polluted." This environmental health change occurred during a lowstand-highstand sea-level transition during the mid-Holocene.

It is important to remember that these overall changes in the environmental health of the lagoon are interpreted to be a response of benthic foraminifera to "improvements" in the evolutionary change of oxygenation from anoxic to less suboxic conditions (Fig. 9a) since the sediments in this interval are not anthropogenically polluted with PTEs (low PLI and SPI; Fig. 7). Also, we can deduce that the stressing conditions were a consequence of accumulation and degradation of organic matter. It is speculated that the organic matter supplied to the study area should have been of good quality since the elphidiids are known to feed on various food sources, e.g., diatoms, dinoflagellates, green algae in addition to husbanding their chloroplasts (Correia and Lee 2000; Pillet et al. 2011). Based on Jorissen (1999) model on food and oxygen availability, the conditions in this interval are interpreted to be between mesotrophic-to-eutrophic under a hypoxic zone. This is supported by the predominant epifaunal life mode of elphidiids and due to the increment and availability of nutrients and organic matter allowing the colonization of infaunal organisms such as *B. aculeata* (Jorissen et al. 2018) and A. parkinsoniana as stress-tolerant species (Dimiza et al. 2016) that can be found buried deeper within the sediment layers tolerating oxygen depletion and dysoxia.

Between 114 and 106 cm, the PCA factor 1 and factor 2 show a short-lived episode in which the degree of confinement was lessened ≈ 6.5 –6.3 ka BP suggesting changes in the configuration of the barrier island development as evidenced by a drastic decrease in the feldspar/quartz ratio. It has been reported that between 6.5 and 6.4 ka BP, Sepetiba Bay experienced a marine incursion event in which paleoriver channels were flooded and filled with sediments and delta environments were developed along the eastern portion of the bay (Borges and Nittrouer, 2015). This sudden occurrence of more

open marine conditions should imply better environmental health; however, during this short time interval, H', J', FSI, and Exp(H'bc) values declined abruptly (Fig. 10). Several of the environmental sensitive elphidiids coupled with B. aculeata and B. peruviana reached 0% in their relative abundances. However, C. poeyanum reached its maximum abundance at 110 cm depth, as is commonly found in relatively deeper water settings (e.g., Debenay et al. 2001b) when compared to the shallower water elphidiids (e.g., Culver 1990). The ecological response of foraminifera is a result of salinity changes being theorized that this is the last episode of "normal" marine conditions since from this interval towards the core tope, the degree of confinement increased (PCA factor 1; Fig. 14). In the case of B. aculeata, a possible substrate changes toward coarser sediments (e.g., lower feldspar/ quartz ratio) is responsible for their short-lived disappearance since this species thrive on fine-grained (mud) sediments (Dimiza et al. 2016). In the case of B. peruviana, it has been reported in sandy substrates from proximal to the marine source in modern estuaries in Brazil (e.g., Stevenson et al. 1998; Vilela et al. 2011) but has rarely been recovered from intertidal settings (Cusminsky et al. 2006; Calvo-Marcilese and Pratolongo 2009). The increase in the relative abundance of this species may correspond to phases of better communication with the ocean and is associated with cold water of South Atlantic Central Water (SACW) which can penetrate in coastal areas (Boltovskoy et al. 1980; Lançone et al. 2005).

According to the Exp(H'bc) values, FSI, FD, SR, H', and J' values, the best environmental health conditions recorded in the whole core occurred around $\approx 5-2.5$ ka BP (between 86 and 56 cm). It is concluded that these optimal conditions are related to the transition to the final stages of Sepetiba Bay before becoming an estuary. Sloss et al. (2005) reported that during sea-level stabilization and bay barrier development, the influence of marine currents is minimized and restricted to areas proximal to sandy bay barriers. This could be the case



of Sepetiba Bay where the overall degree of environmental confinement has been increasing except during this time interval where it seemed to reach a natural "equilibrium" (PCA factor 1; Fig. 14) probably due to a developed sand barrier complex that further isolated the bay as explained by Friederichs et al. (2013). This also could explain the rapid decrease in SMGS coupled with an increase in fine sediments (mud) and TOM preservation as a response to a reduction in estuarine water turnover or flushing mechanism which has been described as a change from wave (high-energy) to tidal (low-energy) processes (Fletcher et al. 1990). The estuarine conditions during this period are supported by the first appearance and rapid increase in abundance of B. elegantissima and B. striatula which are well-known taxa to be tolerant to eutrophic settings (Dimiza et al. 2016), whereas C. poeyanum is constantly declining indicative of lower salinity and oxygenation coupled with a rapid substrate change towards organicrich and muddy sediments (Fig. 2).

Anthropized estuarine sedimentary environment (pprox 1975–2015 AD)

The upper 40 cm of the core SP8, which represents the period since ≈ 1975 AD (35–34 cm) after a 1000-year hiatus, was marked by a sharp increase of siltation, anthropogenic PTE pollution, mainly Zn, Cd, As (Fig. 2), and high TOM. During this period, the water column became frequently stratified and, in the sediments, variable suboxic conditions prevailed, as indicated by the Mn values and the EF-Mo/EF-U (Figs. 2, 9a). The exponential increase of the AEI also corroborates the increasing prevalence of suboxic to anoxic conditions in the sediments as the confinement conditions of the Marambaia Cove became relatively stable, whereas in the sediment, it is speculated that oxygen porewater contents tended to be reduced, the Mn profile suggests a trend of increased "oxygenation" as observed in other restricted estuaries (e.g., Martínez-Colón et al. 2017) since Mn precipitates in oxic frontiers.

It is known that U enrichment in sediments, under suboxic-anoxic conditions, occurred when hydrogen sulfides are not present, whereas Mo is associated with hydrogen sulfides or oxidized sediments linked to Mn oxidehydroxides (e.g., Pattan et al. 2019). The slight increase in the Mo/U profile is due to the lower enrichment of Mo over a narrow range of U values (Fig. 9a, b) which can be interpreted as recurring presence-absence of dissolved oxygen or a transient redox boundary. This could be a potential effect of siltation (e.g., variable oxygenation; Pattan et al. 2019) due to 20 million m³ of bay sediments being dredged (Costa Santos et al. 2019), thus altering water circulation, sedimentation, oxygenation, remobilization of sequestered and buried PTEs, and increased preservation of TOM and mud-sized sediments (Molisani et al. 2004; Bastos and Bassani 2012; Díaz Morales et al. 2019). This relationship is not observed between 174 and 150 cm where the environment was fully anoxic and relatively borderline with sulfiderich euxinic conditions at 150 cm (Fig. 9b).

Dredging activities have been reported in other estuaries as having been the cause of sedimentary anoxic conditions as well as the permanent stratification of the water column (e.g., Martínez-Colón et al. 2017, 2018) and to alter the chemistry of the estuary by the mixing of anoxic-suboxic porewaters with oxygenated water creating transient or oscillating oxidizing/reducing conditions (e.g., Audry et al. 2007; Schäfer et al. 2010). These chemical changes indeed affect the fate and transport of PTEs. For example, the respective "significant"-to-"very high" and "significant" enrichments of Cd and Zn during this period is a quite impressive issue. Both PTEs are strongly correlated to their affinity with TOM, CO₃, and mud-sized sediments and when compared to their variability downcore, it is uncanny that the high EF values are due to anthropogenic forcing as this is supported by numerous authors that have reported higher values for Cd and Zn from the surface and core sediments from around the bay (Marques Jr. et al. 2006; Ferreira and Moreira 2015; Araújo et al. 2017a, 2017b; Díaz Morales et al. 2019). Given the current redox conditions of Marambaia Cove between 40 and 0 cm, it is expected that Zn and Cd are coprecipitated with oxide-hydroxides as well as remaining complexed with TOM, adsorbed to clay surfaces and in deeper sediment layers coprecipitated with sulfides, because the system is never fully and well oxygenated. It is important to highlight that the main source of Zn and Cd is of anthropogenic in origin as evidenced by the disposal of industrial waste (Lacerda et al. 1987) and copious amounts of industrial smelting (Gomes et al. 2009; Araújo et al. 2017a, 2017b) as well for As which is used during Zn metallurgy (Magalhães and Pfeiffer 1995), although between 174 and 40 cm, it is inferred that the high concentrations of As is based on natural sources (Baeyens et al. 2019). These anthropic actions resulted in drastic enrichments of Zn and Cd in the order of 26× and 6× higher than pre-industrial respective values (Margues Jr. et al. 2006), or 23× to 8× times, respectively, according to our study. Although a 2.5× enrichment is observed for As, its maximum concentrations are below the 8.2-10-mg/kg⁻¹ background levels (Magalhães and Pfeiffer 1995; CONAMA 2004). In addition to metals, the surface sediments of Marambaia Cove are contaminated by a large amount of microplastic particles. These particles constitute the sedimentary fraction > 500 µm in the core top. The accumulation of microplastic particles is also one of the most recent insights of the anthropogenic influence in the external region of Sepetiba Bay. Research on the occurrence of microplastics in marine settings and organisms through food chains has increased considerably in recent years (for review, see Ivar do Sul and Costa 2014). In Brazil, there has been a growing concern about this type of pollution and the number



of works on the subject has also been increasing recently (ex: Costa et al. 2010; Castro et al. 2018; Neto et al. 2019; Barletta et al. 2019; Garcia et al. 2020) given the great impact caused by this type of pollution on the environment and living organisms. The abundance of microplastics may also be a problem in Sepetiba Bay; however, their influence on the organisms that are part of the initial links in the chains is not yet known, particularly on the foraminifera. From a PTE pollution perspective, the environmental conditions of the lagoon reached its worst at 25 cm (≈ 1986 AD) especially since Zn exceeds level 2 (> 410 mg kg⁻¹; adverse effects) values established by the CONAMA (2004), Brazilian legislation. The sediments and the whole system were considered respectively as "dangerous" and "deteriorated" based on the PSI and PLI values. Conditions improved towards "highly polluted" between 25 and 0 cm as a potential consequence after the end of metallurgical activities in 1998 (e.g., Magalhães and Pfeiffer 1995; Araújo et al. 2017b). However, the lasting effects of these PTEs are still recorded in the sediments. For example, the environmental health of the study area has deteriorated reaching marginal "poor" to "bad" (ExpH'bc; Fig. 10) conditions while remaining "heavily polluted" (FSI; Fig. 14). This is reflected in the ecology of the foraminifers as exemplified by a size reduction in foraminifera (which were found mostly in the sediment fraction 63–125 µm) denoting the occurrence of short life cycles or potential dormancy. Also, the foraminiferal assemblage experienced a monospecific faunal turnover from the dominant C. poeyanum to A. tepida. The latter is an infaunal shallow-water species (Coccioni 2000) that proliferate in euryhaline areas with reduced competition from other species (Murray 1991, 2006) and is known to tolerate reduced oxygenation caused by the high accumulation of organic matter among other stressors (e.g., Boltovskoy 1965). As mentioned earlier, the rapid increase in the Ammonia/Elphidium ratio coincided with a decline in H' and J' and with an increase in mud-sized sediments and TOM which strongly suggests that the degree of confinement in Marambaia Cove has reached "normal" estuarine conditions since then.

Conclusion

The core SP8 constitutes an early Holocene record of the evolution of the Marambaia Cove, in the external sector of Sepetiba Bay, since ≈ 9.5 ka BP. The main phases of this evolution can be summarized as follow:

The study area represents a fuvio-terrestrial paleoenvironment ≈ 9.5–7.8 ka BP that experienced events of dryness (≈ 9.5–8.6 ka BP) and wash over (≈ 8.6–7.8 ka BP). The accumulation of large amounts

- of organic matter induced oxygen depletion and even anoxia in the sediments giving place to biogeochemical processes that resulted in the retention of PTEs, supplied by the weathering of rocks and minerals, increasing the natural sediment toxicity from $\approx 8.3\,$ ka BP. The climatic event 8.2 ka BP in which the South American Summer Monsoon was intensified in Brazil and gave place to higher rainfall and moisture was signed by an anoxic event and increased toxicity of the sediment.
- 2. The study area became a shallow marine environment in the last ≈ 7.8 ka BP: FSI and Exp(H'bc), based on the composition and species ecology of benthic foraminifera assemblages, which suggest that the environmental conditions evolved from bad to more favorable (low PTE enrichment, good connection with oceanic waters); its maximum quality was reached at ≈ 5 ka BP, during the mid-Holocene relative sea-level highstand; since then, the confinement increased progressively, inducing changes in the composition of benthic foraminifera assemblages.
- 3. The environment has been undergoing strong anthropization since ≈ 1975 AD. This recent period was marked by the increase of silting and Cd, Zn, and organic matter contents. The rise of PLI and SPI values, the decreasing of FSI and Exp(H'bc) values (ecological indicators), and the exponential increase of the *Ammonia/Elphidium* values suggest that the environment evolved from "moderately polluted" to "heavily polluted", between ≈ 1975 and 2015 AD. Such bad ecological conditions induced major changes in foraminifera assemblages with a significant reduction of diversity and dominance by *A. tepida*, a stresstolerant species.

The core SP8 also records changes in biotic and abiotic variables probably related to the development of the Marambaia barrier island. The most significant was recorded after 1.2 ka BP when a hydrodynamic event caused the remobilization of a significant portion of the sedimentary record.

Supplementary Information The online version contains supplementary material available at https://doi.org/10.1007/s11356-020-12179-9.

Acknowledgments Dr. Martínez-Colón were provided by the National Science Foundation Geography and Spatial Sciences Program (grant number 1853794). The authors would like to thank the Editor and the anonymous reviewers for the contribution for improving this work. The first author would like to thank her fellowship to Coordenação de Aperfeiçoamento de Pessoal de Nível Superior (CAPES), Brazil. This paper is a contribution of the projects of Conselho Nacional de Desenvolvimento Científico e Tecnológico of Brazil, CnPQ (project process # 443662/2018-5) and Fundação Carlos Chagas Filho de Amparo à Pesquisa do Estado do Rio de Janeiro, FAPERJ (Edital PENSA RIO, process # E-26/010.003024/2014). Virginia Martins would like to thank



the CNPq and FAPERJ for the research grants (processes # 302676/2019-8 and E-26/202.927/2019, respectively). Brazil. Mauro Geraldes would like to thank the CNPq and FAPERJ for the research grants (processes # 301470/2016-2 and E-26/202.843/2017, respectively). The authors would like to thank the Fundação para a Ciência e a Tecnologia (FCT, Portugal; the strategic project UID/GEO/04035/2019; UIDB/04035/2020) for financial support. Dr. Martínez-Colón were provided by the National Science Foundation Geography and Spatial Sciences Program (grant number 1853794).

Authors' contributions All the authors were involved in the work:

Wellen Castelo: data acquisition, performed the experiment analysis, interpretation of data, wrote the paper

Virgínia Martins: data acquisition, analysis or interpretation of data, conceived and designed the experiments, wrote the paper, funding acquisition

Michael Martínez-Colón: wrote the paper

Josefa Guerra: conceived and designed the experiments, wrote the paper

Tatiana Dadalto: data acquisition, performed field trip and sample collections, performed the experiment

Denise Terroso: data acquisition, performed the experiment Maryane Soares: data acquisition, performed the experiment

Fabrizio Frontalini: investigation, wrote the paper

Wânia Duleba: investigation, wrote the paper

Orangel Antonio Aguilera Socorro: investigation, wrote the paper

Mauro Cesar Geraldes: investigation, funding acquisition

Fernando Rocha: investigation, funding acquisition

Sergio Bergamaschi: investigation

Funding W. Castello received a fellowship by the Coordenação de Aperfeiçoamento de Pessoal de Nível Superior (CAPES), Brazil. This work received financial contributions from Conselho Nacional de Desenvolvimento Científico e Tecnológico of Brazil, CnPQ (project process # 443662/2018-5), Fundação Carlos Chagas Filho de Amparo à Pesquisa do Estado do Rio de Janeiro, FAPERJ (Edital PENSA RIO, process # E-26/010.003024/2014) and Fundação para a Ciência e a Tecnologia (FCT, Portugal; the strategic project UID/GEO/04035/2019; UIDB/04035/2020). Virginia Martins received research grants from CNPq and Fundação Carlos Chagas Filho de Amparo à Pesquisa do Estado do Rio de Janeiro, FAPERJ (processes # 302676/2019-8 and E-26/202.927/2019). Mauro Geraldes received research grants from CNPq and Fundação Carlos Chagas Filho de Amparo à Pesquisa do Estado do Rio de Janeiro, FAPERJ (processes # 301470/2016-2 and E-26/202.843/2017, respectively).

Data availability All data and materials are available in the manuscript and as supplementary materials.

Compliance with ethical standards

Competing interests The authors declare that they have no competing interest.

Ethical approval The work follows the stated ethical principles. The work is based on original material and was not and will be not published elsewhere in any form or language (partially or in full), unless the new work concerns an expansion of previous work.

Consent to participate The authors have permissions for the use of materials and software.

Consent to publish The authors approved the version to be published.



References

- Aberner RA (1984) Sedimentary pyrite formation: an update. Geochim Cosmochim Acta 48(4):605–615. https://doi.org/10.1016/0016-7037(84)90089-9
- Alegría H, Martínez-Colón M, Kurt-Karakus P, Brooks G, Hanson L, Birgul A (2016) Historical sediment record and levels of PCBs in sediments and mangroves of Jobos Bay, Puerto Rico. Sci Total Environ 573:1003–1009
- Algeo TJ, Tribovillard N (2009) Environmental analysis of paleoceanographic systems based on molybdenum–uranium covariation. Chem Geol 268(3–4):211–225. https://doi.org/10.1016/j.chemgeo.2009.09.001
- Ali H, Khan E, Ilahi I (2019) Environmental chemistry and ecotoxicology of hazardous heavy metals: environmental persistence, toxicity, and bioaccumulation. J Chem 6730305:14. https://doi.org/10.1155/ 2019/6730305
- Alve E (1991) Benthic foraminifera in sediment cores reflecting heavy metal pollution in Sørfjord, western Norway. J Foraminifer Res 21: 1–19. https://doi.org/10.2113/gsjfr.21.1.1
- Alves Martins MV, Pereira E, Figueira RCL, Oliveira T, Pinto Simon AFS, Terroso D, Ramalho JCM, Silva L, Ferreira C, Geraldes MC, Duleba W, Rocha F, Rodrigues MA (2019a) Impact of eutrophication on benthic foraminifera in Sepetiba Bay (Rio de Janeiro State, SE Brazil). J Sedimentary Environ 4(4):480–500. https://doi.org/10. 12957/jse.2019
- Alves Martins MV, Hohenegger J, Frontalini F, Sequeira C, Miranda P, Rodrigues MAC, Duleba W, Laut L, Rocha F (2019b) Foraminifera check list and the main species distribution in the Aveiro Lagoon and Adjacent Continental Shelf (Portugal). J Sedimentary Environ 4(1):1–52. https://doi.org/10.12957/jse.2019.39308
- Alves Martins MV, Pinto AFS, Borghi L, Carelli TG, Morlote M, Rey D, Pereira E, Ramalho JCR, Rocha F, Geraldes M, Potratz GL, Duleba W, Reis AT, Guerra JV, Rodrigues MAC (2020) Influence of the Holocene relative sea level on the coastal plain of Sepetiba Bay (Southeast Brazil). J Sedimentary Environ 5(1):35–59. https://doi.org/10.1007/s43217-019-00002-6
- Angulo RJ, Lessa GC (1997) The Brazilian sea level curves: a critical review with emphasis on the curves from Paranaguá and Cananéia regions. Mar Geol 140:141–166. https://doi.org/10.1016/S0025-3227(97)00015-7
- Araújo DF, Peres LGM, Yepez S, Mulholland DS, Machado W, Tonhá M, Garnier J (2017a) Assessing man-induced environmental changes in the Sepetiba Bay (Southeastern Brazil) with geochemical and satellite data. Compt Rendus Geosci 349:290–298. https://doi.org/10.1016/j.crte.2017.09.007
- Araújo DF, Boaventura GR, Machado W, Viers J, Weiss D, Patchineelam SR, Ruiz I, Rodrigues APC, Babinski M, Dantas E (2017b) Tracing of anthropogenic zinc sources in coastal environments using stable isotope composition. Chem Geol 449:226–235. https://doi.org/10.1016/j.chemgeo.2016.12.004
- Armynot du Chatelet E, Bout-Roumazeilles V, Coccioni R, Frontalini F, Francescangeli F, Margaritelli G, Rettori R, Spagnoli F, Semprucci F, Trentesaux A, Tribovillard N (2016) Enironmental control on a land-sea transitional setting: integrated sedimentological, geochemical and faunal approaches. Environ Earth Sci 75(123):1–18. https://doi.org/10.1007/s12665-015-4957-7
- Arunakumara KKIU, Walpola BC, Yoon M-H (2013) Current status of heavy metal contamination in Asia's rice lands. Rev Environ Sci Biotechnol 12(4):355–377. https://doi.org/10.1007/s11157-013-9323-1
- Audry S, Blanc G, Schäfer J, Robert S (2007) Effect of estuarine sediment resuspension on early diagenesis, sulfide oxidation and dissolved molybdenum and uranium distribution in the Gironde estuary,

- France. Chem Geol 238:149–167. https://doi.org/10.1016/j.chemgeo.2006.11.006
- Aylagas E, Borja A, Irigoien X, Rodriguez-Ezpeleta N, 2016. Benchmarking DNA metabarcoding for biodiversity-based monitoring and assessment. Front Mar Sci, 10. https://doi.org/10.3389/fmars.2016.00096
- Baeyens W, Mirlean N, Bundschuh J, Winter N, Baisch P, Silva Júnior FMR, Gao Y (2019) Arsenic enrichment in sediments and beaches of Brazilian coastal waters: a review. Sci Total Environ 681:143– 154. https://doi.org/10.1016/j.scitotenv.2019.05.126
- Barcellos C, Lacerda LD, Ceradini S (1997) Sediment origin and budget in Sepetiba Bay (Brazil) an approach based on multi-element analysis. Environ Geol 32:203–209
- Barletta M, Lima ARA, Costa MF (2019) Distribution, sources and consequences of nutrients, persistent organic pollutants, metals and microplastics in South American estuaries. Sci Total Environ 651: 1199–1218
- Bastos BC, Bassani C, 2012. A questão da expansão portuária como solução para o desenvolvimento econômico: o caso das dragagens e os impactos ambientais na baía de Sepetiba. Simpósio de Excelência em Gestão e Tecnologia, 17 p.
- Biscaye P (1965) Mineralogy and sedimentation of recent deep-sea clay in the Atlantic Ocean and adjacent seas and oceans. GSA Bull 76(7): 803–832. https://doi.org/10.1130/0016-7606(1965)76[803: MASORD]2.0.CO;2
- Boltovskoy E (1965) Los Foraminiferos Recientes: biologia, métodos de estúdio, aplicación oceanográfica. EUDE-BA, Buenos Aires, p 510
- Boltovskoy E, Giussani G, Watanabe S, Wright R, 1980. Atlas of benthic shelf foraminifera to the southwest Atlantic. New York, The Hague, 174 p.
- Borges HV, Nittrouer CA (2015) The paleo-environmental setting of sepetiba bay, Rio de Janeiro, Brazil, in the late pleistocene: Interpretations from high-resolution seismic stratigraphy. Revista Brasileira de Geofísica 33(3):1–14
- Borges HV, Nittrouer CA (2016) Sediment accumulation in Sepetiba Bay during the Holocene: a reflex of the human influence. J Sedimentary Environ 1(1):90–106. https://doi.org/10.12957/jse.2016.21868
- Bouchet VMP, Alve E, Rygg B, Telford RJ (2012) Benthic foraminifera provide a promising tool for ecological quality assessment of marine waters. Ecol Indic 23:66–75. https://doi.org/10.1016/j.ecolind.2012. 03.011
- Bouchet VMP, Gobervilleb E, Frontalini F (2018) Benthic foraminifera to assess Ecological Quality Statuses in Italian transitional waters. Ecol Indic 84:130–139. https://doi.org/10.1016/j.ecolind.2017.07. 055
- Brönnimann P, Moura JA, Dias-Brito D (1981a) Estudos Ecológicos na Baía de Sepetiba, Rio de Janeiro, Brasil: Foraminíferos. In: In: Congresso Latino-Americano de Paleontologia. RS, Porto Alegre, pp 75–861
- Brönnimann P, Moura JA, Dias-Brito D, 1981b. Foraminíferos da Fácies Mangue da Planície de Maré de Guaratiba, Rio de Janeiro, Brasil. In: Congresso Latino-Americano de Paleontologia, Porto Alegre, RS, pp. 91-861.
- Buat-Menard P, Chesselet R (1979) Variable influence of the atmospheric flux on the trace metal chemistry of oceanic suspended matter. Earth Planet Sci Lett 42:398–411. https://doi.org/10.1016/0012-821X(79) 90049-9
- Bueno C, Figueira R, Ivanoff MD, Toldo Junior EE, Fornaro L, García-Rodríguez FG (2019) A multi proxy assessment of long-term anthropogenic impacts in Patos Lagoon, southern Brazil. J Sedimentary Environ 4(3):276–290. https://doi.org/10.12957/jse. 2019.44612
- Calvo-Marcilese L, Pratolongo P (2009) Foraminíferos de marismas y llanuras de marea del estuario de Bahía Blanca, Argentina: distribución e implicaciones ambientales. Rev Esp Micropaleontol 41:315–332

- Carelli SG, Roncarati H, Nascimento DN, Geraldes MC (2011) Síntese da evolução Geológica Cenozoica da Baía de Sepetiba e Restinga de Marambaia, Sul do Estado do Rio de Janeiro. XIII ABEQUA Congress – The South American Quaternary: Challenges and Perspectives.
- Castro JWA, Suguio K, Seoane JCS, Cunha AM, Dias FF (2014) Sealevel fluctuations and coastal evolution in the state of Rio de Janeiro, southeastern Brazil. An Acad Bras Cienc 86(2):671–683. https://doi.org/10.1590/0001-3765201420140007
- Castro RO, Silva ML, Araújo FV (2018) Review on microplastic studies in Brazilian aquatic ecosystems. Ocean Coast Manag 165:385–400. https://doi.org/10.1016/j.ocecoaman.2018.09.013
- Chakravarty R, Banerjee PC (2008) Morphological changes in an acidophilic bacterium induced by heavy metals. Extremophiles 12:279– 284. https://doi.org/10.1007/s00792-007-0128-4
- Chen H-F, Yeh P-Y, Song S-R, Hsu S-C, Yang T-N, Wang Y, Chi Z, Lee T-Q, Chen M-T, Cheng C-L, Zou J, Chang Y-P (2013) The Ti/Al molar ratio as a new proxy for tracing sediment transportation processes and its application in aeolian events and sea level change in East Asia. J Asian Earth Sci 73:31–38. https://doi.org/10.1016/j.jseaes.2013.04.017
- Cheng H, Fleitmann D, Edwards LR, Wang X, Cruz FW, Auler AS, Mangini A, Wang Y, Kong X, Burns SJ, Matter A (2009) Timing and structure of the 8.2 kyr B.P. event inferred from δ18O records of stalagmites from China, Oman, and Brazil. Geology 37:1007–1010. https://doi.org/10.1130/G30126A.1
- Coates DR (ed) (1973) Coastal geomorphology. State University of New York Publications in Geomorphology, Binghamton, p 404
- Coccioni R (2000) Benthic foraminifera as bioindicators of heavy metal pollution a case study from the Goro Lagoon (Italy). In: Martin RE (ed) Environmental micropaleontology: the application of microfossils to environmental geology. Kluwer Academic/Plenum Publishers, New York, pp 71–103
- CONAMA Conselho Nacional do Meio Ambiente (2004). Resolução N° 344, de 25 de Março de 2004, Publicada no DOU n° 087, de 07/ 05/2004, pp. 56-57.
- Copeland G, Monteiro T, Couche S, Borthwickd (2003) Water quality in Sepetiba Bay, Brazil. Mar Environ Res 55:385–408. https://doi.org/10.1016/S0141-1136(02)00289-1
- Correia M, Lee JJ (2000) Chloroplast retention by *Elphidium excavatum* (Terquem). Is it a selective process? Symbiosis 29(4):343–355
- Costa Santos CS, Dias FF, Franz B, Santos PR, Rodrigues T, Vargas R, Américo dos Santos C (2019) Relative sea level rise effects at the Marambaia Barrier Island and Guaratiba Mangrove: Sepetiba Bay (SE Brazil). J Sedimentary Environ 4(3):249–262. https://doi.org/10.12957/jse.2019.44397
- Costa MF, Ivar do Sul JA, Santos-Cavalcanti JS, Araújo MCB, Spengler A, Tourinho TS (2010) Small and microplastics on the strandline: snapshot of a Brazilian beach. Environ Monit Assess 168:299–304. https://doi.org/10.1007/s10661-009-1113-4
- Culver SJ (1990) Benthic foraminifera of Puerto Rican mangrove-lagoon systems: potential for paleoenvironmental interpretations. Palaios 5(1):34–51
- Cunha CLN, Rosman PCC, Monteiro TCN, 2001. Caracterização da Circulação Bidimensional da Baía de Sepetiba. In: XIV Simpósio Brasileiro de Recursos Hídricos e do V Simpósio de Hidráulica e Recursos Hídricos dos Países de Língua Oficial Portuguesa. Aracaju-SE: ABRH, vol. 1, p. 151-151.
- Cunha CLN, Rosman PCC, Ferreira AP, Monteiro TCN (2006) Hydrodynamics and water quality models applied to Sepetiba Bay. Cont Shelf Res 26:1940–1953. https://doi.org/10.1016/j.csr.2006. 06.010
- Cusminsky GC, Martínez D, Bernasconi E (2006) Foraminíferos y ostrácodos de sedimentos recientes del estuario de Bahía Blanca, Argentina. Rev Esp Micropaleontol 38:395–410



- Dadalto TP, (2017). arquitetura estratigráfica e evolução geológica da Restinga da Marambaia (RJ). PhD thesis, Universidade Federal Fluminense, Niterói – RJ, Brazil, 273 p.
- Dantas M (2000) Geomorfologia do Estado do Rio de Janeiro. Ministério De Minas e Energia, Secretaria de Minas e Metalurgia. CPRM – Serviço Geológico do Brasil, Brasília. https://doi.org/10.13140/RG. 2.2.32582.57923
- Debenay J-P, Eichler BB, Duleba W, Bonetti C, Eichler-Coelho P (1998) Water stratification in coastal lagoons: its influence on foraminiferal assemblages in two Brazilian lagoons. Mar Micropaleontol 35:67–98. https://doi.org/10.1016/S0377-8398(98)00011-5
- Debenay J-P, Duleba W, Bonetti C, Melo-E-Souza SH, Eichler BB (2001a) *Pararotalia cananeiaensis* n. sp., indicator of marine influence and water circulation in Brazilian coastal and paralic environments. J Foraminifer Res 31:152–163
- Debenay JP, Geslin E, Eichler BB, Duleba W, Sylvestre F, Eichler P (2001b) Foraminiferal assemblages in a hypersaline lagoon, Araruama (R.J.) Brazil. J Foraminifer Res 31(2):133–151. https://doi.org/10.2113/0310133
- Dias MI, Prudêncio MI (2008) On the importance of using scandium to normalize geochemical data preceding multivariate analyses applied to archaeometric pottery studies. Microchem J 88:136–141. https://doi.org/10.1016/j.microc.2007.11.009
- Dias-Brito D, Moura J, Wurding N (1988) Relationships between ecological models based on ostracodes and foraminifers from Sepetiba Bay (Rio de Janeiro Brazil). In: Hanai, T. et al. (ed.). Evolutionary biology of Ostracoda: its fundamentals and applications. Dev Paleontol Stratrigraphy 11:467–485
- Díaz Morales SJ, Guerra JV, Nunes MAS, Souza AM, Geraldes MC (2019) Evaluation of the environmental state of the western sector of Sepetiba Bay (SE Brazil): trace metal contamination. J Sedimentary Environ 4(2):174–188. https://doi.org/10.12957/jse. 2019.43764
- Dimiza MD, Triantaphyllou MV, Koukousioura O, Hallock P, Simboura N, Karageorgis AP, Papathanasiou E (2016) The Foram Stress Index: a new tool for environmental assessment of soft-bottom environments using benthic foraminifera. A case study from the Saronikos Gulf, Greece, Eastern Mediterranean. Ecol Indic 60: 611–621. https://doi.org/10.1016/j.ecolind.2015.07.030
- Dolven JK, Alve E, Rygg B (2013) Defining past ecological status and in situ reference conditions using benthic foraminifera: a case study from the Oslofjord, Norway. Ecol Indidicators 29:219–233. https://doi.org/10.1016/j.ecolind.2012.12.031
- Duleba W, Teodoro AC, Debenay J-P, Alves Martins MV, Gubitoso S, Pregnolato LA, Lerena LM, Prada SM, Bevilacqua JAE (2018) Environmental impact of the largest petroleum terminal in SE Brazil: a multiproxy analysis based on sediment geochemistry and living benthic foraminifera. PLoS One 13(2):e0191446. https://doi. org/10.1371/journal.pone.0191446
- Duque MM, Giacomini J, Wasserman JC (2008) Modelagem hidrodinâmica bidimensional da Baía da Ilha Grande e Baía de Sepetiba visando a subsidiar o plano local de desenvolvimento da maricultura. In: XX Semana Nacional de Oceanografia, 2008, Arraial do Cabo - RJ. CD de Resumos. Rio de Janeiro: Faculdade de Oceanografia – UERJ, p. 1-3.
- Elliott M, Quintino V (2007) The estuarine quality paradox, environmental homeostasis and the difficulty of detecting anthropogenic stress in naturally stressed areas. Mar Pollut Bull 54(6):640–645. https://doi.org/10.1016/j.marpolbul.2007.02.003
- Fagel N, 2007. Clay minerals, deep circulation and climate. Developments in marine geology, Volume 1, Elsevier B.V., pp. 139-184. ISSN 1572-5480, https://doi.org/10.1016/S1572-5480(07)01009-3
- Ferreira AP, Moreira MDFR (2015) Metals pollution status in surface sediments along the Sepetiba Bay Watershed, Brazil. J Coast Zone Manag. https://doi.org/10.4172/2473-3350.1000404

- Fletcher CH, Knebel HJ, Krat J (1990) Holocene evolution of an estuarine coast and tidal wetlands. GSA Bull 102(3):283–297
- Folk RL, Ward WC (1957) Brazos River bar: a study in the significance of grain size parameters. J Sediment Petrol 27:3–26. https://doi.org/10.1306/74D70646-2B21-11D7-8648000102C1865D
- Franzo A, Roscioli C, Patrolecco L, Bzzaro M, Del Negro P, Cibic T (2019) Influence of natural and anthropogenic disturbances of foraminifera and free living nematods in four lagoons of the Po delta system. Estuar Coast Shelf Sci 220:99–110. https://doi.org/10.1016/j.ecss.2019.02.039
- Friederichs YL, Reis AT, Silva CG, Toulemonde B, Guerra JV (2013)
 Arquitetura Sísmica do Sistema Fluvio-estuarino da Baía de
 Sepetiba Preservado na Estratigrafia Rasa da Plataforma Interna
 Adjacente, Rio de Janeiro. Braz J Geol 43(1):124–138. https://doi.
 org/10.5327/Z2317-48892013000100011
- Garcia M, Campos CC, Mota EMT, Santos NMO, Campelo RPS, Prado LCG, Melo Junior M, Soares MO (2020) Microplastics in subsurface waters of the western equatorial Atlantic (Brazil). Mar Pollut Bull 150:110705. https://doi.org/10.1016/j.marpolbul.2019.110705
- Geraldes MC, Motoki A, Costa A, Mota CE, Mohriak WU (2013) Geochronology (Ar/Ar and K-Ar) of the South Atlantic postbreak-up magmatism. Geol Soc Spec Publ 369:1–34
- Geraldes MC, Souza AM, Mane MA, Salomão MS, Silva C, Tavares AD, Silva DA, Santos AC, Cézar AD, Almeida PMM (2017) Alkaline complexes as potential areas for installation of repositories of nuclear waste: Cretaceous intrusions in Brazil. J Sedimentary Environ 1(2):111–132. https://doi.org/10.12957/jse.2017.30051
- Gomes FC, Godoy JM, Godoy MLDP, Carvalho ZL, Lopes RT, Sanchez-Cabeza JA, Lacerda LD, Wasserman JC (2009) Metal concentrations, fluxes, inventories and chronologies in sediments from Sepetiba and Ribeira Bays: A comparative study. Mar Pollut Bull 59:123–133. https://doi.org/10.1016/j.marpolbul.2009.03.015
- Gutierrez MT, Dadalto TP, Morales SJD, Cortez RHC, Guerra JV, Geraldes MC, 2011. Estudo preliminar da variação de parâmetros físicos da água ao longo de dois ciclos de maré na Baía de Sepetiba (RJ), Brasil XIII Congresso da Associação Brasileira de Estudos do Quaternário ABEQUA.
- Hayes MO (1967) Hurricanes as geological agents: case studies of hurricanes Carla, 1961, and Cindy, 1963, University of Texas. Bur Econ Geol Pub 61:56
- Hem JD 1985. USGS Water Supply paper n. 2254, 3rd edition. 263 p. Hermans SM, Buckley HL, Case BS, Curran-Cournane F, Taylor M, Lear G (2017) Bacteria as emerging indicators of soil condition. Appl Environ Microbiol. https://doi.org/10.1128/AEM.02826-16
- Hess S, Alve E, Andersen TJ, Joranger T (2020) Defining ecological reference conditions in naturally stressed environments - how difficult is it? Mar Environ Res 156:104885. https://doi.org/10.1016/j. marenvres.2020.104885
- Hippensteel SP, Martin RE (1999) Foraminifera as an indicator of overwash deposits, barrier island sediment supply, and barrier island evolution: Folly Island, South Carolina. Palaeogeogr Palaeoclimatol Palaeoecol 149:115–125
- Hofer G, Wagreich M, Neuhuber S (2013) Geochemistry of fine-grained sediments of the upper Cretaceous to Paleogene Gosau Group (Austria, Slovakia): implications for paleoenvironmental and provenance studies. Geosci Front 4:449–468
- Hogg AG, Hua Q, Blackwell PG, Niu M, Buck CE, Guilderson TP, Heaton TJ (2013) Southern Hemisphere calibration, 0–50,000 years cal BP. Radiocarbon 55(4):1889–1903
- Ivar do Sul JA, Costa MF (2014) The present and future of microplastic pollution in the marine environment. Environ Pollut 185:352–364. https://doi.org/10.1016/j.envpol.2013.10.036
- Jesus PB, Dias FF, Muniz RA, Macário KCD, Seoane CS, Quattrociocchi DGS, Cassab RCT, Aguilera O, Souza RCCL, Alves EQ, Chanca IS, Carvalho CRA, Araujo JC (2017) Holocene paleo-sea level in southeastern Brazil: an approach based on vermetids shells. J



- Sedimentary Environ 2(1):35-48. https://doi.org/10.12957/jse. 2017.28158
- Jorissen FJ (1999) Benthic foraminiferal microhabitats below the sediment-water interface. In: Sen Gupta BK (ed) Modern foraminifera. Kluwer Academic Publishers, Boston, pp 191–179
- Jorissen F, Nardelli MP, Almogi-Labin A, Barras C, Bergamin L, Bicchi E, El Kateb A, Ferraro L, McGann M, Morigi C, Romano E, Sabbatini A, Schweizer M, Spezzaferri S (2018) Developing Foram-AMBI for biomonitoring in the Mediterranean: species assignments to ecological categories. Mar Micropaleontol 140:33–45. https://doi.org/10.1016/j.marmicro.2017.12.006
- Krumbein WC, Pettijohn F (1938) Manual of sedimentary petrology. Appleton Century-Crofts, New York
- Kuniansky EL, and Rodríguez JM, 2010. Effects of changes in irrigation practices and aquifer development on groundwater discharge to the Jobos Bay National Estuarine Research Reserve near Salinas, Puerto Rico. U.S. Geological Survey Scientific Investigations Report 2010-5022, 106p.
- Lacerda LD, Pfeiffer WC, Fiszman M (1987) Heavy metal distribution, availability and fate in Sepetiba Bay, SE Brazil. Sci Total Environ 65:163–173. https://doi.org/10.1016/0048-9697(87)90169-0
- Lacerda LD, Marins RV, Paraquetti HHM, Mounier S, Benaim J, Fevrier D (2001) Mercury distribution and reactivity in waters of a subtropical coastal lagoon, Sepetiba Bay, SE Brazil. J Braz Chem Soc 12(1):93–98. https://doi.org/10.1590/S0103-50532001000100013
- Lai MY, Shen PP, Zhao Z, Zhou H, Gu JD (2005) Concentrations of heavy metals in the benthic microgastropods Sermyla riqueti and Stenothyra devalis at the Mai Po Inner Deep Bay Ramsar site of Hong Kong. Bull Environ Contam Toxicol 74(6):1065–1071. https://doi.org/10.1007/s00128-005-0689-9
- Lançone RB, Duleba W, Mahiques MM (2005) Dinâmica de fundo da enseada do flamengo, Ubatuba, Brasil, inferida a partir da distribuição espacial, morfometria e tafonomia de foraminíferos. Revista Brasileira de Paleontologia 8(3):181–192
- Larson RA, Brooks GR, Devine B, Schwing PR, Holmes CW, Jilert T, Reichart G-J (2015) Elemental signature of terrigenous sediment runoff as recorded in coastal salt ponds: US Virgin Islands. Appl Geochem 63:573–585. https://doi.org/10.1016/j.apgeochem.2015. 01.008
- Laut LLM, Silva FS, Martins, V., Rodrigues MAC, Mendonça JO, Clemente IMMM, Laut VM, Mentzigen G (2012) Foraminíferos do Complexo Sepetiba/Guaratiba. In: Baía de Sepetiba: Estado da Arte. Rodrigues, M.A.C., Pereira, S.D., Santos, S.B., Rio de Janeiro: Cobã, pp. 115 - 150.
- Laut LLM, Martins MVA, Frontalini F, Belart P, Santos VF, Lorini ML, Fortes RR, Silva FS, Vieira SSS, Souza-Filho PWM (2016) Biotic (foraminifera and thecamoebians) and abiotic parameters as proxies for indication of the environmental heterogeneity in Caeté River Estuary, Amazon Coast, Brazil. J Sedimentary Environ 1(1):1–16. https://doi.org/10.12957/jse.2016.21264
- Lessa GC, Meyers SR, Marone E (1998) Holocene stratigraphy in the Paranagua Bay estuary, southern Brazil. *J Sediment Res* 68(6): 1060–1076. https://doi.org/10.2110/jsr.68.1060
- Loeblich AR Jr, Tappan H, (1964). Sarcodina, chiefly Thecamoebians and Foraminiferida. In: R. C. Moore (Ed.), Treatise on invertebrate paleontology, Geological Society of America, vol. 1, pp. 1-510, vol. 2, pp. 511-900, University of Kansas Press.
- Loeblich AR, Tappan H (1988) Foraminiferal genera and their classification. Van Nostrand Reinhold, New York, 970 pp
- Loring DH (1988) Normalization of heavy metal data. Report of the 75th Statutory Meeting of WGMS in Relation to Pollution, Annex 2 edn. ICES Publications, Copenhagen, pp 19–42
- Loring DH, Rantala RTT (1992) Manual for the geochemical analyses of marine sediments and suspended particulate matter. Earth-Sci Rev 32:238–282. https://doi.org/10.1016/0012-8252(92)90001-A

- Lu B, Li T, Yu X, Chang F, Nan Q (2011) Redox conditions in sediments and during sedimentation in the Ontong Java Plateau, west equatorial Pacific. Chin J Oceanogr Limnol 29:1309–1324
- Macario KD, Alves EQ, Belém AL, Aguilera O, Bertucci T, Tenório MC, Oliveira FM, Chanca IS, Carvalho C, Souza R, Scheel-Ybert R, Nascimento GS, Dias F, Caon J (2018) The marine reservoir effect on the coast of rio de janeiro: deriving ΔR values from fish otoliths and mollusk shells. Radiocarbon 2018:1–18. https://doi.org/10.1017/RDC.2018.23
- Magalhães VF, Pfeiffer WC (1995) Arsenic concentration in sediments near a metallurgical plant (Sepetiba Bay, Rio de Janeiro, Brazil). J Geochem Explor 52(1–2):175–181
- Magurran AE (1988) Ecological diversity and its measurement. University Press, Princeton
- Marques AN Jr, Monna F, Silva Filho EV, Fernex FE, Simões Filho FFL (2006) Apparent discrepancy in contamination history of a subtropical estuary evaluated through ²¹⁰Pb profile and chronostratigraphical markers. Mar Pollut Bull 52:532–539. https://doi.org/10.1016/j.marpolbul.2005.09.048
- Martínez-Colón M, Hallock P (2010) Preliminary survey on foraminiferal responses to pollutants in Torrecillas Lagoon, Puerto Rico. Caribb J Sci 46(1):106–111. https://doi.org/10.2113/gsjfr.39.4.278
- Martínez-Colón M, Hallock P, Green-Ruíz C (2009) Strategies for using shallow-water foraminifers as bioindicators of potentially toxic elements: a review. J Foraminifer Res 39(4):278–299
- Martínez-Colón M, Hallock P, Green-Ruíz C, Smoak J (2017) Temporal variability in potentially toxic elements (PTE's) and benthic foraminifera in an estuarine environment in Puerto Rico. Micropaleontology 63(6):357–381
- Martínez-Colón M, Hallock P, Green-Ruíz C, Smoak J (2018) Benthic foraminifera as bioindicators of potentially toxic elements (PTE) pollution: Torrecilla Lagoon, Puerto Rico. Ecol Indicators J 89: 516–527. https://doi.org/10.1016/j.ecolind.2017.10.045
- Martins V, Dubert J, Jouanneau J-M, Weber O, Silva EF, Patinha C, Alveirinho Dias JM, Rocha F (2007) A multiproxy approach of the Holocene evolution of shelf–slope circulation on the NW Iberian Continental Shelf. Mar Geol 239:1–18. https://doi.org/10. 1016/j.margeo.2006.11.001
- Matero ISO, Gregoire LJ, Ivanovic RF, Tindall JC, Haywood AM (2017)
 The 8.2 ka cooling event caused by Laurentide ice saddle collapse.
 Earth Planet Sci Lett 473:205–214. https://doi.org/10.1016/j.epsl.
 2017.06.011
- Mc Granaham G, Balk D, Anderson B (2007) The rising tide: assessing the risks of climate change and human settlements in low elevation coastal zones. Environ Urban 19(1):17–37. https://doi.org/10.1177/0956247807076960
- Miranda LB, Ikeda, Yoshimine I, Castro Filho BM, Pereira Filho N (1977) Note on the occurrence of saline fronts in the Ilha Grande (RJ) region. Boletim do Instuto Oceanográfico 26(2):249–256. https://doi.org/10.1590/S0373-55241977000200003
- Miselis JL, Andrews BD, Nicholson RS, Defne Z, Ganju NK, Navoy A (2016) Evolution of mid-Atlantic coastal and back-barrier estuary environments in response to a hurricane: implications for barrierestuary connectivity. Estuar Coasts 39:916–934. https://doi.org/10. 1007/s12237-015-0057-x
- Misumi S, de Barros M, Vilela C, Barth O (2014) Palinologia, Paleoflorística e Aspectos Paleoclimáticos de Sedimentos do Pleistoceno Tardio na Bacia Hidrográfica do Rio Guandu, Rio de Janeiro, Brasil. Anu Inst Geocienc 37:104–114. https://doi.org/10. 11137/2014 1 104 114
- Molisani MM, Marins RV, Machado W, Paraquetti HHM, Bidone ED, Lacerda LD (2004) Environmental changes in Sepetiba Bay, SE Brasil. Reg Environ Chang 4:17–27
- Morrill C, LeGrande AN, Renssen H, Bakker P, Otto-Bliesner BL (2013) Model sensitivity to North Atlantic freshwater forcing at 8.2 ka. Clim Past 9:955–968. https://doi.org/10.5194/cp-9-955-2013



- Murray JW (1991) Ecology e paleoecology of benthic foraminifera. Logman Scientific & Technical, London, p 397
- Murray JW (2006) Ecology and applications of benthic foraminifera. Cambridge University Press, Cambridge, p 426
- Nascimento DN, Chaves HAF, Carelli SC, Polivanov H, Geraldes MC (2013) Caracterização paleoambiental utilizando argilas costeiras de Subsuperfície Estudo de caso: Baía de Sepetiba-RJ. In: Rodrigues MAC, Pereira SD, Bergamaschi S (eds) Interações Homem-Meio nas zonas costeiras: Brasil/Portugal, vol 1, 1ª edn. Corbã, Rio de Janeiro, pp 281–282
- Nascimento DN, Salomão MS, Mane MA, Geraldes MC, Alves Martins MV (2019) Marine progression records in the Sepetiba Bay region (RJ-Brazil) by GPR and ground magnetic survey. J Sedimentary Environ 4(4):518–539. https://doi.org/10.12957/jse.2019.47382
- Neto JAB, Gaylarde C, Beech I, Bastos AC, Quaresma VS, Carvalho DG (2019) Microplastics and attached microorganisms in sediments of the Vitória bay estuarine system in SE Brazil. Ocean Coast Manag 169:247–253. https://doi.org/10.1016/j.ocecoaman.2018.12.030
- Neumann B, Vafeidis AT, Zimmermann J, Nicholls RJ (2015) future coastal population growth and exposure to sea-level rise and coastal flooding - a global assessment. PLoS One 10(3):e0118571. https:// doi.org/10.1371/journal.pone.0118571
- Olabarria C (2002) Role of colonization in spatio-temporal patchiness of micrograstropods in coralline turf habitat. J Exp Mar Biol Ecol 274: 121–140. https://doi.org/10.1016/S0022-0981(02)00201-0
- PARH Guandu (Plano de ação de recursos hídricos da unidade de análise Guandu), (2010). Plano integrado de recursos hídricos da bacia do Rio Doce e dos planos de ações de recursos hídricos para as unidades de planejamento e gestão de recursos hídricos no âmbito da Bacia do Rio Doce. Consórcio ECOPLAN LUME, Contrato N° 043/2007 IGAM.
- Patchineelam S, Sanders C, Smoak J, Zem R, Oliveira G, Patchineelam S (2011) A historical evaluation of anthropogenic impact in coastal ecosystems by geochemical signatures. J Braz Chem Soc 22:120–125. https://doi.org/10.1590/S0103-50532011000100016
- Pattan JN, Parthiban G, Amonkar A (2019) Productivity controls on the redox variation in the southeastern Arabian Sea sediments during the past 18 kyr. Quat Int 523:1–9. https://doi.org/10.1016/j.quaint.2019. 05.034
- Pillet L, Vargas C, Pawlowski J (2011) Molecular identification of sequestered diatom chloroplasts and kleptoplastidy in foraminifera. Protist 162(3):394–404. https://doi.org/10.1016/j.protis. 2010.10.001
- Pinto AFS, Martins MVA, Rodrigues MAC, Nogueira L, Laut LLM, Pereira E (2016) Late Holocene evolution of the Northeast intertidal region of Sepetiba Bay, Rio de Janeiro (Brazil). J Sedimentary Environ 1(1):107–138. https://doi.org/10.12957/jse.2016.21924
- Pinto AFS, Martins MVA, Fonseca MCM, Pereira E, Terroso DL, Rocha F, Rodrigues MAC (2017) Late Holocene closure of a barrier beach in Sepetiba Bay and its environmental impact (Rio de Janeiro, Brazil). J Sedimentary Environ 2(1):65–80. https://doi.org/10.12957/jse.2017.28215
- Prazeres M, Martínez-Colón M, Hallock P (2020) Foraminifera as bioindicators of water quality: the FoRAM Index revisited. Environ Pollut 257:113612. https://doi.org/10.1016/j.envpol.2019. 113612
- Pregnolato LA, Viana RA, Passos CC, Misailidis ML, Duleba W (2018) *Ammonia-Elphidium* Index as a proxy for marine pollution assessment, Northeast Brazil. J Sedimentary Environ 3(3):176–186. https://doi.org/10.12957/jse.2018.38001
- Ramakrishna A, Gill SS (Eds), 2019. Metabolic adaptations in plants during abiotic stress. CRC Press, Taylor & Francis Group.
- Raposo DS, Laut VM, Clemente IMMM, Martins MVA, Frontalini F, Silva FS, Lorini ML, Fortes RR, Laut LLM (2016) Recent benthic foraminifera from the Itaipu Lagoon, Rio de Janeiro (southeastern Brazil). Check List 12(5):1–14. https://doi.org/10.15560/12.5.1959

- Reis AT, Amendola G, Dadalto TP, Silva CG, Poço RGT, Guerra JV, Martins V, Cardia RR, Gorini C, Rabineau M (2020) Arquitetura e Evolução Deposicional da Sucessão Sedimentar Pleistoceno Tardio-Holoceno (últimos ~20 ka) da Baía de Sepetiba (RJ). São Paulo, UNESP. Geociências 39(3):695–708 ISSN: 1980-900X
- Rico KI, Sheldon ND, Gallagher TM, Chappaz A (2019) Redox Chemistry and Molybdenum Burial in a Mesoproterozoic Lake. Geophys Res Lett 46(11):5871–5878. https://doi.org/10.1029/ 2019GL083316
- Rodrigues MA, Pereira SD, Araújo-Junior HI, Pereira ONA (2018) Contexto geológico da Baía de Sepetiba, Estado do Rio de Janeiro in: Baía de Sepetiba - Riscos à natureza e aos coletivos humanos na metrópole do Rio de Janeiro. pp. 228, 1ª Ed., Letra Capital.
- Rodrigues SK, Machado W, Guerra JV, Geraldes M, Morales S, Vinzóna SB (2020) Changes in Cd and Zn distribution in sediments after closure of an electroplating industry, Sepetiba bay, Brazil. Mar Pollut Bull 161:111758. https://doi.org/10.1016/j.marpolbul.2020. 111758
- Roncarati H, Carelli SG (2012) Considerações sobre o Estado da Arte dos Processos Geológicos Cenozóicos Atuantes na Baía de Sepetiba. In: Rodrigues MAC, Pereira SD, Santos SB (eds) Baía de Sepetiba: Estado da Arte. Corbã, Rio de Janeiro, pp 13–36
- Sallun AEM, Sallun Filho W, Suguio K, Babinski M, Gioia SMCL, Harlow BA, Duleba W, Oliveira PE, Garcia MJ, Weber CZ, Christofoletti SR, Santos CS, Medeiros VB, Silva JB, Santiago-Hussein MC, Fernandes RS (2012) Geochemical evidence of the 8.2 ka event and other Holocene environmental changes recorded in paleolagoon sediments, southeastern Brazil. Quat Res 77:31–43. https://doi.org/10.1016/j.yqres.2011.09.007
- Schäfer J, Castelle S, Blanc G, Dabrin A, Masson M, Lanceleur L, Bossy C (2010) Mercury methylation in the sediments of a macrotidal estuary (Gironde Estuary, south-west France). Estuar Coast Shelf Sci 90(2):80–92. https://doi.org/10.1016/j.ecss.2010.07.007
- Schmidt GA, LeGrande AN (2005) The Goldilocks abrupt climate change event. Quat Sci Rev 24:1109–1110. https://doi.org/10.1016/j.quascirev.2005.01.015
- SEMADS (Secretaria de Estado do Meio Ambiente e Desenvolvimento Sustentável, Estado do Rio de Janeiro) 2001. Bacias Hidrográficas e Rios Fluminenses. Síntese Informativa por Macrorregião Ambiental. Cooperação Técnica Brasil-Alemanha, Projeto PLANÁGUA SEMADS/GTZ, Rio de Janeiro, 73 p. ISBN 85-87206-10-9
- Semensatto-Jr DL, Dias-Brito D (2004) Análise ambiental de uma área parálica no delta do Rio São Francisco, Sergipe-Brasil, com base na sinecologia de foraminíferos e tecamebas (Protista). Revista Brasileira de Paleontologia 7:53–66
- Sen Gupta BK, Turner RE, Rabalais NN (1996) Seasonal oxygen depletion in continental-shelf waters of Louisiana: historical record of benthic foraminifers. Geology 24(3):227–230. https://doi.org/10.1130/0091-7613(1996)024<0227:SODICS>2.3.CO,2
- Shannon CE (1948) A mathematical theory of communication. Bell Syst Tech J 27:379–423
- Silva JB, Duleba W, Sallun AM, Suguio K (2014) Benthic foraminifera as evidence of paleoenvironmental changes between 9400 and 8300 cal YBP at the Juréia-Itatins Ecological Station paleolagoon (SP, Brasil). J Coast Res 30(6):1118–1130. https://doi.org/10.2112/ JCOASTRES-D-12-00121.1
- Silva MAM, Souza MFL, Abreu PC (2015) Spatial and temporal variation of dissolved inorganic nutrients, and chlorophyll-a in a tropical estuary in northeastern Brazil: dynamics of nutrient removal. Braz J Oceanogr 63(1):1–15. https://doi.org/10.1590/S1679-87592015064506301
- Singh M, Müller G, Singh IB (2002) Heavy metals in freshly deposited stream sediments of rivers associated with urbanisation of the Ganga Plain, India. Water Air Soil Pollut 141:25–54. https://doi.org/10.1023/A:1021339917643



- Sinha R, Raymahashay BC (2004) Evaporite mineralogy and geochemical evolution of the Sambhar Salt Lake, Rajsthan, India. Sediment Geol 166:59–71. https://doi.org/10.1016/j.sedgeo.2003.11.021
- Sloss CR, Jones BG, Murray-Wallace CV, Mc-Clennen CE (2005) Holocene sea level fluctations and the evolution of a barrier estuary: Lake Illawarra, New SouthWales, Australia. J Coast Res 21:943–959
- Smith CJ, Collins LS, Hayek L-EC (2013) Biogeographic effects of the closing central American seaway on benthic foraminifera of Venezuela. Bull Mar Sci 89(3):921–936
- Stevenson MR, Dias-Brito D, Stech JL, Kampel M (1998) How do cold water biota arrive in a tropical bay near Rio de Janeiro, Brazil? Cont Shelf Res 18:1959–1612. https://doi.org/10.1016/S0278-4343(98) 00029-6
- Stuiver, M., Reimer, P.J., Reimer, R.W., 2020, CALIB 7.1 [WWW program] at http://calib.org, accessed 2020-5-4
- Stuvier M, Reimer PJ (1993) Extended ¹⁴C data base and revised CALIB 3.0 ¹⁴C age calibration. Radiocarbon 35:215–230. https://doi.org/10.1017/S0033822200013904
- Suguio K, Vieira EM, Barcelo JH, Silva MS (1979) Interpretação ecológica dos foraminíferos de sedimentos modernos da Baía de Sepetiba e adjacencias. Rio de Janeiro. Revista Brasileira de Geociências 9(4):233–247
- Sutherland RA (2000) Bed sediment-associated trace metals in an urban stream, Oahu, Hawaii. Environ Geol 39:611–627. https://doi.org/10.1007/s002540050473
- Taheri M, Grego M, Riedel B, Vincx M, Vanaverbeke J (2015) Patterns in nematode community during and after experimentally induced anoxia in the northern Adriatic Sea. Mar Environ Res 10:110–123
- Thomas ER, Wolff EW, Mulvaney R, Steffensen JP, Johnsen SJ, Arrowsmith C, White JWC, Vaughn B, Popp T (2007) The 8.2 ka event from Greenland ice cores. Quat Sci Rev 26:70–81. https://doi.org/10.1016/j.quascirev.2006.07.017
- Tinoco IM (1967) Contribuição da sedimentologia e microfauna da Baia de Sepetiba (Estado do Rio de Janeiro). Trabalhos Oceanográficos da Universidade Federal de Pernambuco. Recife 7(8):123–136
- Tomlinson DL, Wilson JG, Harris CR, Jeffrey DW (1980) Problems in the assessment of heavy-metal levels in estuaries and the formation of a pollution index. Helgoländer Meeresun 33:566–575. https://doi. org/10.1007/BF02414780

- Trindade MI, Rocha F, Dias MI (2010) Geochemistry and mineralogy of clays from the Algarve Basin, Portugal: a multivariate approach to palaeoenvironmental investigations. Curr Anal Chem 6:43–52
- Tupinambá M, Heilbron M, Duarte BP, Nogueira JR, Valladares C, Almeida J, Silva LGE, Medeiros SR, Almeida CG, Miranda A, Ragatky CD, Mendes J, Ludka I (2007) Geologia da Faixa Ribeira Setentrional: Estado da arte e conexões com a Faixa Araçuaí. Geonomos 15(1):67–79
- Turekian KK, Wedepohl KH (1961) Distribution of the elements in some major units of the Earth's crust. Geol Soc Am Bull 72: 175–192. https://doi.org/10.1130/0016-7606(1961)72[175: DOTEIS]2.0.CO;2
- Vilela CG, Batista DS, Neto JAB, Ghiselli RO (2011) Benthic foraminifera distribution in a tourist lagoon in Rio de Janeiro, Brazil: a response to anthropogenic impacts. Mar Pollut Bull 62(10):2055–2074. https://doi.org/10.1016/j.marpolbul.2011.07.023
- Waśkowska A, Kaminski MA (2019) Pleistocene epilithic foraminifera from the Arctic Ocean. PeerJ 7:e7207. https://doi.org/10.7717/peerj. 7207
- Wedepohl K (1995) The composition of the continental crust. Geochim Cosmochim Acta 59:1217–1232. https://doi.org/10.1016/0016-7037(95)00038-2
- Wolanski, E., Day, J.W., Elliott, M., Ramesh, R. (Editors), (2009). Coasts and estuaries: the future. Elsevier.
- Zaninetti L, Brönnimann P, Beurlen G, Moura JA, (1976). La mangrove de Guaratiba et la Baie de Sepetiba, Etat de Rio de Janeiro, Bresil: Foraminiferes et ecólogie. Note préliminaire, C.R. des Seances, PSHN Geneve, NS, 11, 39-44
- Zaninetti L, Brönnimann P, Beurlen G, Moura JA (1977) La mangrove de Guaratiba et la Baie de Sepetiba, Etat de Rio de Janeiro, Bresil: Foraminiferes et ecólogie. Arch Sci 30(2):161–178
- Zhao M-Y, Zheng Y-F (2015) The intensity of chemical weathering: geochemical constraints from marine detrital sediments of Triassic age in South China. Chem Geol 391:111–122. https://doi.org/10.1016/j.chemgeo.2014.11.004

Publisher's note Springer Nature remains neutral with regard to jurisdictional claims in published maps and institutional affiliations.

Affiliations

Wellen Fernanda Louzada Castelo ¹ • Maria Virgínia Alves Martins ^{2,3} • Michael Martínez-Colón ⁴ • • Josefa Varela Guerra ⁵ • • Tatiana Pinheiro Dadalto ⁶ • Denise Terroso ³ • Maryane Filgueiras Soares ² • Fabrizio Frontalini ⁷ • • Wânia Duleba ⁸ • Orangel Antonio Aguilera Socorro ⁹ • Mauro Cesar Geraldes ² • • Fernando Rocha ³ • • Sergio Bergamaschi ²

- Programa Pós-Graduação em Dinâmica dos Oceanos e da Terra, Universidade Federal Fluminense, UFF, Campus da Praia Vermelha, Niterói. RJ. Brazil
- Faculdade de Geologia, Universidade do Estado do Rio de Janeiro, Av. São Francisco Xavier, 524, sala 2020A, Maracanã, Rio de Janeiro, RJ 20550-013, Brazil
- Departamento de Geociências, Universidade de Aveiro, GeoBioTec, Campus de Santiago, 3810-193 Aveiro, Portugal
- Florida A and M University, School of the Environment, FSH Science Research Center, 1515 South MLK Blvd, Tallahassee, FL 32307, USA

- Faculdade de Oceanografia, Universidade do Estado do Rio de Janeiro, UERJ, Rua São Francisco Xavier, 524, 4° andar, Bloco E, sala 4018, Rio de Janeiro, RJ 20550-900, Brazil
- Universidade Federal do Sul da Bahia UFSB, Rodovia de Acesso para Itabuna, km 39 - Ferradas, Itabuna, BA 45613-204, Brazil
- Dipartimento di Scienze Pure e Applicate (DiSPeA), Università degli Studi di Urbino "Carlo Bo", Urbino, Italy
- Escola de Artes, Ciências e Humanidades, Universidade de São Paulo, São Paulo, SP, Brazil



Terms and Conditions

Springer Nature journal content, brought to you courtesy of Springer Nature Customer Service Center GmbH ("Springer Nature").

Springer Nature supports a reasonable amount of sharing of research papers by authors, subscribers and authorised users ("Users"), for small-scale personal, non-commercial use provided that all copyright, trade and service marks and other proprietary notices are maintained. By accessing, sharing, receiving or otherwise using the Springer Nature journal content you agree to these terms of use ("Terms"). For these purposes, Springer Nature considers academic use (by researchers and students) to be non-commercial.

These Terms are supplementary and will apply in addition to any applicable website terms and conditions, a relevant site licence or a personal subscription. These Terms will prevail over any conflict or ambiguity with regards to the relevant terms, a site licence or a personal subscription (to the extent of the conflict or ambiguity only). For Creative Commons-licensed articles, the terms of the Creative Commons license used will apply.

We collect and use personal data to provide access to the Springer Nature journal content. We may also use these personal data internally within ResearchGate and Springer Nature and as agreed share it, in an anonymised way, for purposes of tracking, analysis and reporting. We will not otherwise disclose your personal data outside the ResearchGate or the Springer Nature group of companies unless we have your permission as detailed in the Privacy Policy.

While Users may use the Springer Nature journal content for small scale, personal non-commercial use, it is important to note that Users may not:

- 1. use such content for the purpose of providing other users with access on a regular or large scale basis or as a means to circumvent access control:
- 2. use such content where to do so would be considered a criminal or statutory offence in any jurisdiction, or gives rise to civil liability, or is otherwise unlawful:
- 3. falsely or misleadingly imply or suggest endorsement, approval, sponsorship, or association unless explicitly agreed to by Springer Nature in writing:
- 4. use bots or other automated methods to access the content or redirect messages
- 5. override any security feature or exclusionary protocol; or
- 6. share the content in order to create substitute for Springer Nature products or services or a systematic database of Springer Nature journal content

In line with the restriction against commercial use, Springer Nature does not permit the creation of a product or service that creates revenue, royalties, rent or income from our content or its inclusion as part of a paid for service or for other commercial gain. Springer Nature journal content cannot be used for inter-library loans and librarians may not upload Springer Nature journal content on a large scale into their, or any other, institutional repository.

These terms of use are reviewed regularly and may be amended at any time. Springer Nature is not obligated to publish any information or content on this website and may remove it or features or functionality at our sole discretion, at any time with or without notice. Springer Nature may revoke this licence to you at any time and remove access to any copies of the Springer Nature journal content which have been saved.

To the fullest extent permitted by law, Springer Nature makes no warranties, representations or guarantees to Users, either express or implied with respect to the Springer nature journal content and all parties disclaim and waive any implied warranties or warranties imposed by law, including merchantability or fitness for any particular purpose.

Please note that these rights do not automatically extend to content, data or other material published by Springer Nature that may be licensed from third parties.

If you would like to use or distribute our Springer Nature journal content to a wider audience or on a regular basis or in any other manner not expressly permitted by these Terms, please contact Springer Nature at

 $\underline{onlineservice@springernature.com}$